

**Analysis, Modeling, and Prediction of Infrasound
and Low Frequency Noise from
Wind Turbine Installation**

Phase 1: PEI Site

Final Report

**Please note that, in accordance with the
provisions of the *Access to Information and
Privacy Act* these documents have been
redacted to protect confidential business
information and the identity of study
participants.**

MG Acoustics
IPF M-50
1200 Montreal Road
Ottawa, Ontario
K1A 0R6

February 2014

MG-HC 3

I. INTRODUCTION

Analysis, modeling, and prediction of infrasound and low frequency noise from wind turbines at two different sites is to be carried out as part of a study investigating potential health effects for individuals living at varying distances from wind turbine installations.

This work will allow Health Canada to evaluate whether or not infrasound and/or low frequency noise (from wind turbines in the locations specified) can be detected at different distances; and secondly to determine whether the Parabolic Equation method of calculation gives an adequate explanation of the experimental values with regards to infrasound and/low frequency and distances at which it can be detected. Thirdly, the work being completed will allow Health Canada to reliably make infrasound and low frequency noise predictions (using Harmonoise) with respect to the southern Ontario site.

The work will be completed in 2 phases:

1st Phase – Analysis of infrasound and low frequency noise measurements and analysis of meteorological data will be completed including the generation of theoretical predictions at the PEI site.

2nd Phase – Modeling will be carried out and applied to wind turbines sites in southern Ontario.

An interim report "Analysis, Modeling, and Prediction of Infrasound and Low Frequency Noise from Wind Turbine Installation. Interim Report" was submitted in March 2013. It covered items *a* to *f* of the 1st Phase, as listed in the Statement of Work. A second interim report was submitted in November 2013, incorporating the first interim report and covering the remaining items *g* to *m* of the 1st Phase.

This current Final Report on the 1st Phase (PEI) incorporates the earlier interim reports, recent analysis of noise propagation during wintertime, and comments provided by the Expert Committee.

In this report, there are several objectives:

- investigate the use of Harmonoise/Nord2000 weather classes with Environment Canada weather data to predict sound speed profiles
- investigate methods to separate low-frequency wind turbine noise from other sources of noise
- investigate the directivity of wind turbine noise sources at infrasonic frequencies
- compute wind turbine noise sound pressure levels at long range using state-of-the-art methods [e.g., Parabolic Equation (PE) and Fast Field Program (FFP)], to guide Health Canada in their use of Harmonoise P2P for predicting wind turbine noise propagation
- compare these numerical predictions to experimental results extracted from measurements under a variety of meteorological conditions

An independent report will be submitted describing the 2nd Phase (Southern Ontario) work.

II. [REDACTED] WIND TURBINES

A. Location of [REDACTED] Wind Turbines

There are [REDACTED] wind turbines located [REDACTED] of the [REDACTED] [REDACTED]. Their locations are indicated on the map (ref. [1]) in Figure 1 and numbered [REDACTED]. (Apparently, the [REDACTED] [REDACTED] now numbers these turbines differently.) In the present report, the wind turbines will be designated T1, T2, T3, and T4 as shown here. Reference 1 provides additional detail about this wind farm site.

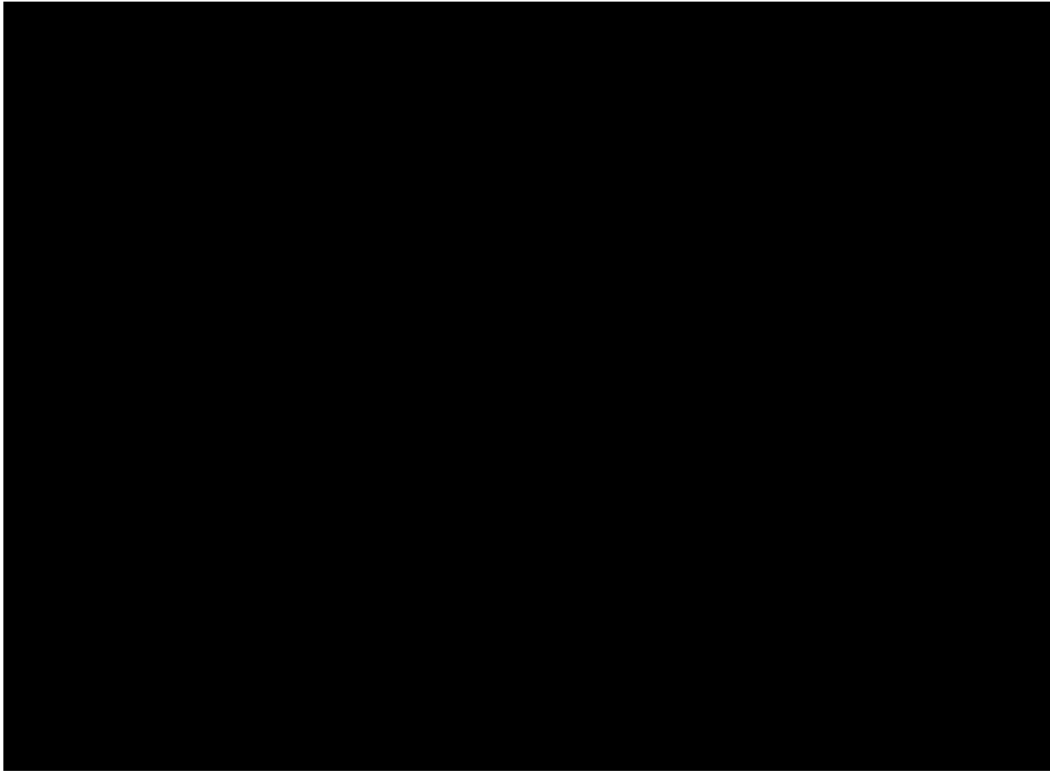


FIG. 1. Map showing location of [REDACTED] wind turbines

The (latitude, longitude) of the four wind turbines is as follows:

[REDACTED]	[REDACTED]
------------	------------

B. Operational Characteristics Relevant to Noise Generation

For analysis of the low frequency noise generated by the wind turbines, there are a few characteristics that are relevant. It is known that one source of noise is the periodic passage of the wind turbine blades. This is infrasound, with the fundamental frequency equal to the blade

passage frequency. The [REDACTED] wind turbines maintain the rotation speed of the blades within a tight range. For wind speeds below approximately 5 m/s, at the height of the rotor, the turbines enter an “idling” mode for which the rotor is not allowed to drop below 10 RPM -- with 3 blades, this gives a minimum blade passage frequency of 0.5 Hz. For wind speeds greater than approximately 8 m/s, the rotational rate is limited: the rotor is not allowed to turn faster than about 16 RPM, giving a maximum blade passage frequency of 0.8 Hz. For wind speeds between 5 m/s and 8 m/s, the rotational rate varies in proportion to the wind speed. It can be anticipated that the generated noise will be evident as a fundamental that varies between 0.5 Hz and 0.8 Hz and its harmonics.

There are other mechanisms of noise generation, gearbox noise for example, which will be broadband. Separating these components from other sources of noise or the ambient background may be challenging.

The [REDACTED] wind turbines are constantly oriented so that the blades face the incoming wind. Any directivity of a noise generation mechanism would be specified relative to the orientation of the blades.

C. Noise output of a [REDACTED]-[REDACTED] MW Wind Turbine

The A-weighted equivalent continuous sound levels of the [REDACTED]-[REDACTED] MW wind turbine [reference 3] are shown in Table 1 as a function of wind speed for octave band frequencies between 25 and 100 Hz.

TABLE 1. L_{Aeq} (dB) as a function of wind speed

Freq (Hz)	6 m/s	7 m/s	8 m/s	9 m/s	10 m/s
25	13.1	15.2	23.7	22.6	22.0
31.5	35.1	38.1	37.6	37.9	38.5
40	34.0	39.6	40.6	40.9	40.9
50	26.3	44.2	46.5	47.0	46.7
63	37.5	39.9	40.2	40.8	40.8
80	36.1	37.8	40.8	41.4	40.5
100	34.6	36.6	42.9	43.0	41.8

The sound levels, as a function of wind direction relative to propagation direction [reference 3], are shown in Figure 2.

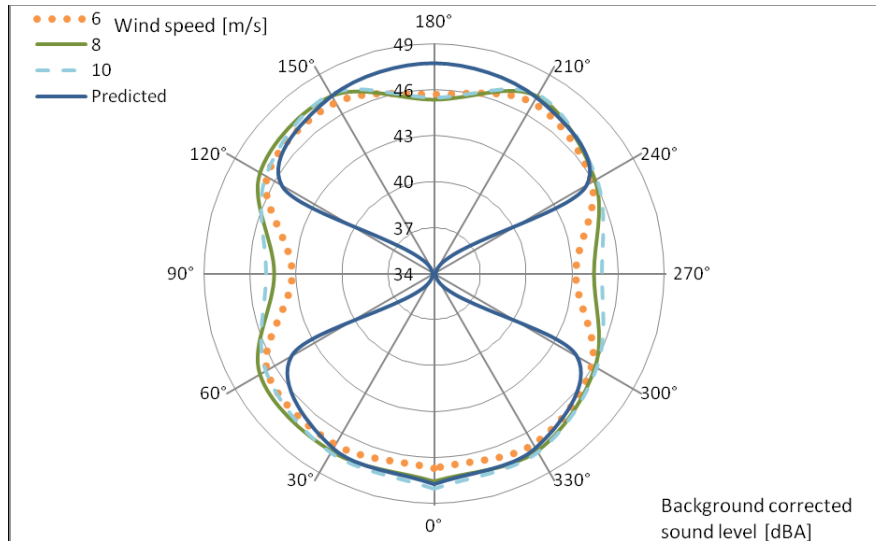


FIG. 2. Horizontal directionality of a wind turbine

There is some variation of sound level with direction although not as large as the predicted response.

III. SELECTION OF MEASUREMENT SITES

Propagation distances of up to 10 km are of interest to this study. There are [REDACTED] wind turbines located at the [REDACTED], PEI site. They are located [REDACTED]. Therefore, an area of about 25 x 25 km surrounding [REDACTED] was considered in the selection of the physical site where infrasound and low frequency noise monitoring will take place. The objective in selecting measurement sites is to have an array of measurement stations along a line extending 10 km from the wind turbines with downwind conditions prevailing as much as possible. The size and shape of Prince Edward Island lead to constraints on the possible locations.

A. Prevailing winds

The highest Sound Pressure Levels (SPL) from the wind turbines are expected to occur directly downwind. Therefore, from Environment Canada records for [REDACTED], PEI, hourly records for one year (2011) were analysed. The Relative Prevalence of different wind directions is shown in the polar plot in Figure 3 below.

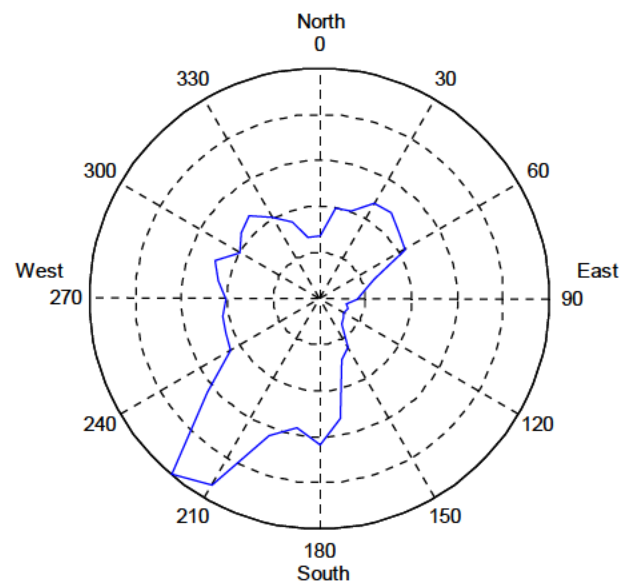


FIG. 3. Relative prevalence of wind direction at [REDACTED]

The wind direction is defined by Environment Canada as the direction from which the wind is coming, with 0° corresponding to north (an east wind, i.e., a wind from the east, would then have an angle 90°).

It is apparent that the prevailing wind direction for the [REDACTED] PEI weather station is [REDACTED] $^\circ$. Unfortunately, this direction runs straight into [REDACTED]. This is indicated by the arrow on the map shown below in Figure 4. Thus, setting up a line of measurement stations in this direction would not give the desired 10 km range.

The polar plots shows that there are very little prevailing winds blowing to the west of [REDACTED] (wind direction of [REDACTED]°).

There are two other directions showing some prevalence; these are around [REDACTED]°. In the direction of [REDACTED]° the lands mass runs into the [REDACTED] before [REDACTED] km is reached. This leaves the area in the general direction to the east of [REDACTED] and the wind turbines for the installation of monitoring array sensors.

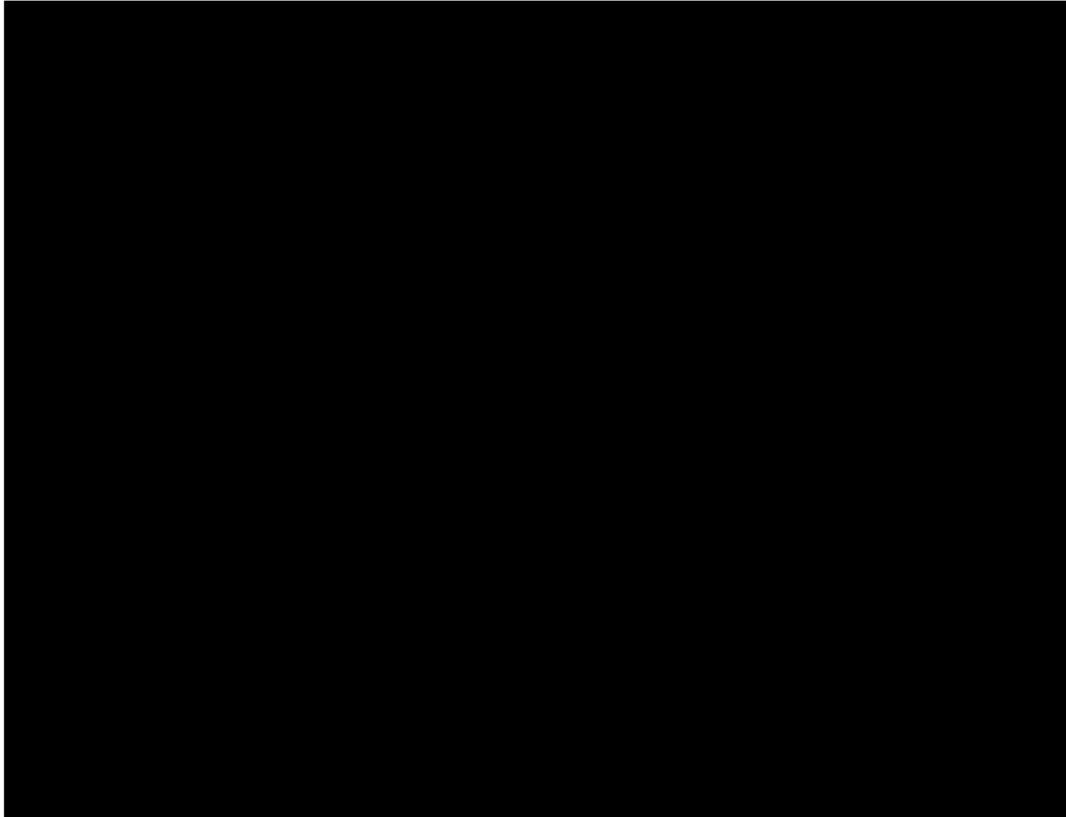


FIG. 4. Map of [REDACTED] wind farm showing prevailing wind direction

B. Locations for Installation of Sensors

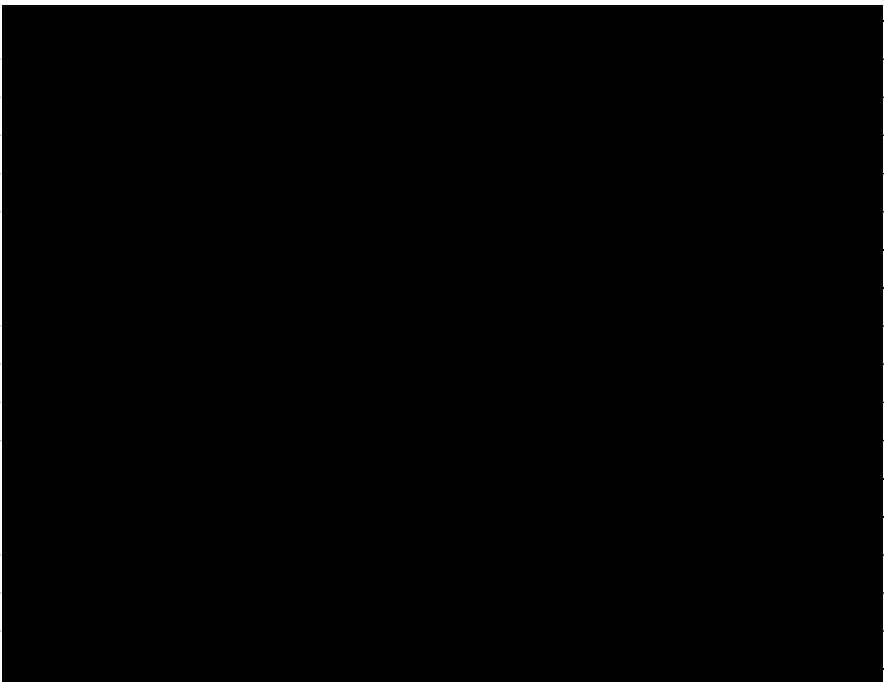
A meeting was held with Health Canada and Natural Resources Canada (NRCan) to determine the specific locations for the installation of infrasound & LFN monitoring array sensors. The placement of NRCan's 4 array sensors was agreed to be at 125 meters, 2.5 km, 5 km and 10 km. In addition, a met tower was to be erected at the 2.5 km location.


The map and PID numbers (property id numbers) on the 10 km map near the [REDACTED] wind farm installation were identified in terms of which properties would be feasible for placement of sensors. Most or all of the properties identified were large rural fields which were privately owned, and in one case, owned by the city with some of the fields possibly owned by large corporations. The placement of the sensors were selected so they were not near bodies of water, major roads or towns in order to keep noise interference to a minimum and also taking into

account prevailing winds in the area. Installation will be battery operated with solar panels used for re-charging purposes; therefore no DC power outlet is needed.

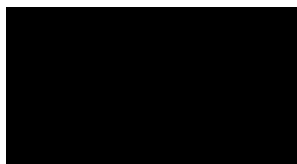
The following are the PIDs and property locations selected as possible sites at the 4 distances (in order of preference in some cases):

TABLE 2. Property ID numbers

Distance	PID	Property location
125 m		
2.5 km		
5 km		
10 km		

Ultimately, NRCan installed four acoustical measurement stations. They are located approximately 125 m, 2.5 km, 5 km, and 10 km from turbine  and are designated HC1P, HC2P, HC3P, and HC4P, respectively. The (latitude, longitude) of the stations is:

HC1P:
 HC2P:
 HC3P:
 HC4P:



A plot of the locations of these four measurement stations and the four wind turbines is shown in Figure 5 below. Wind turbine T2 is used as the origin of the local coordinate system. The meteorological station is located near HC2P.

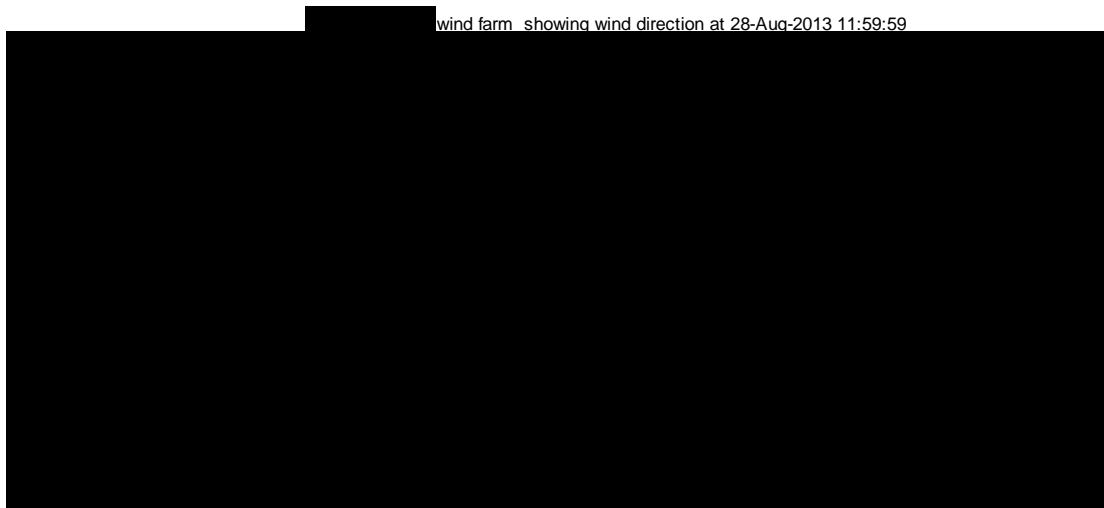


FIG. 5. Relative locations of the four wind turbines (T1, T2, T3, T4) and the four measurement stations (HC1P, HC2P, HC3P, HC4P)

IV. SOURCES OF ACOUSTICAL AND METEOROLOGICAL DATA

Information was available from several sources.

The main source of meteorological data was a meteorological station erected on site by Natural Resources Canada (NRCan)¹. This data was used to compute the sound speed variation with height above ground, a key function needed for calculation of noise propagation. Recognizing that similar meteorological stations may not be available at other sites, an alternate approach was investigated for which Environment Canada weather archives are used to infer sound speed profiles.

The main source of acoustical data was an array of measurement stations deployed by NRCan. Health Canada provided supplementary data measured onsite over several days.

A. Environment Canada Weather Archives

Matlab code was written to collect hourly meteorological data from the Environment Canada website archives. The required data includes temperature, wind direction and speed, and cloud cover.

This information will be used to evaluate a weather station-based approach for determining sound speed profiles. This approach, to be discussed more in Section VI, requires knowledge of the cloud cover for assignment of a stability class. Unfortunately, cloud cover data is not available at the [REDACTED] weather station. Therefore, it was necessary to collect data from other stations not too far away. The weather stations at [REDACTED] NB, [REDACTED], PEI, and [REDACTED], NB, were selected. When the cloud cover is consistent between these three locations, it may be assumed that the cloud cover in [REDACTED] is the same.

A sample of the collected data is shown in Figure 6 below. For each hour of the day, we see temperature, wind speed, and wind direction, all measured at a height of 10 m, for the four weather stations. Temperatures are in degrees Celcius. Wind speeds have been converted to m/s. Wind direction indicates the direction from which the wind is blowing, relative to north (so 90° signifies a wind coming from the east).

¹ For details on the NRCan instrumentation, Health Canada should be contacted.

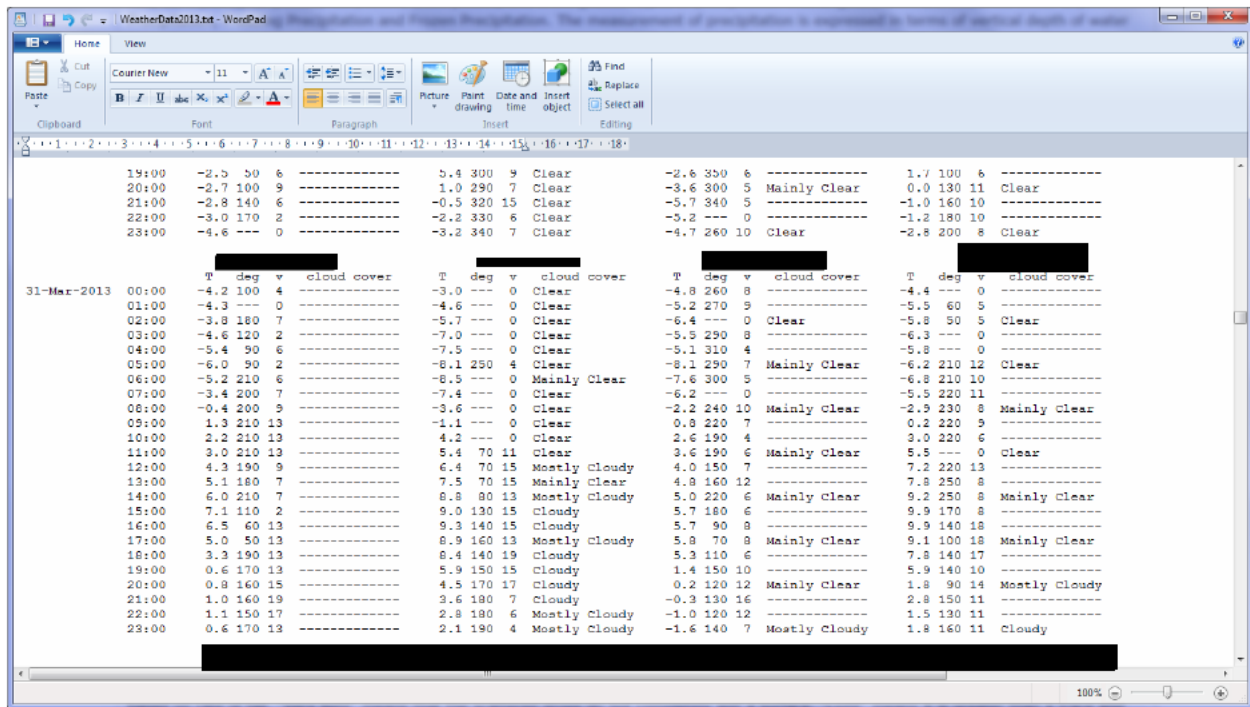


FIG. 6. Sample of weather data from the Environment Canada online archive

The values reported correspond to average readings over the two minutes preceding the hour. The cloud cover indicators correspond to the fraction of sky covered, as defined by:

0/10 : Clear
 1/10 - 4/10 : Mainly Clear
 5/10 - 9/10 : Mostly Cloudy
 10/10 : Cloudy

It should be evident from this example that the weather and, in particular, the cloud cover can be quite different at the different weather stations even though they are not that far apart (_____, _____, and _____). As well, it is seen that the cloud cover can change very rapidly, e.g., from “Clear” to “Mostly Cloudy” over just an hour. A careful screening procedure is needed before a cloud cover can be assigned to _____.

It will also be noted from Figure 6 that cloud cover (when available) is reported hourly at the _____ weather station but only every three hours (02:00, 05:00, ... 23:00) at the _____ and _____ stations. As a result, two alternative schemes were used to estimate the _____ cloud cover based on the time of day.

Suppose, as an example, that the _____ cloud cover is desired for 14:00 on 6 July 2013. As seen in Figure 7 below, this is a time where all three of _____, _____, and _____ stations reported cloud cover; all reported “Mostly Cloudy”. To be quite sure that _____ would have this same cloud cover, we check the _____ data one hour before and one hour later

and we check the [REDACTED] and [REDACTED] data three hours before and three hours later -- these tests are indicated by the gray shading on the figure. In this case, we conclude with some certainty that [REDACTED] would have been “Mostly Cloudy” at 14:00. At this time, the temperature was 31.4° and the wind was 19 m/s from an angle of 250°.

06-Jul-2013					07-Jul-2013				
Time	T	deg	v	cloud cover	Time	T	deg	v	cloud cover
22:00	23.2	270	9	Clear	20:00	20.0	230	7	Clear
23:00	22.0	220	13	Clear	21:00	22.9	260	11	Clear
00:00	21.7	240	11	Clear	22:00	22.0	240	11	Clear
01:00	21.7	250	13	Clear	23:00	21.6	240	11	Clear
02:00	21.4	250	11	Clear	00:00	21.2	240	11	Clear
03:00	21.5	260	13	Clear	01:00	20.7	240	11	Clear
04:00	21.2	260	9	Clear					
05:00	20.0	260	9	Mainly Clear					
06:00	21.8	270	13	Mainly Clear					
07:00	23.8	270	15	Mainly Cloudy					
08:00	25.1	270	15	Mainly Cloudy					
09:00	25.9	270	17	Mainly Cloudy					
10:00	27.7	250	15	Mainly Cloudy					
11:00	27.7	270	13	Mainly Cloudy					
12:00	30.2	240	13	Mainly Cloudy					
13:00	30.1	240	19	Mainly Cloudy					
14:00	31.4	250	19	Mainly Cloudy					
15:00	30.3	240	15	Mainly Cloudy					
16:00	29.4	220	13	Mainly Clear					
17:00	28.1	200	13	Mainly Clear					
18:00	27.3	230	13	Mainly Clear					
19:00	26.0	220	15	Clear					
20:00	23.9	220	15	Clear					
21:00	23.0	230	13	Clear					
22:00	22.1	230	15	Clear					
23:00	21.6	240	11	Clear					

FIG. 7. Selection of weather data used to infer cloud cover at [REDACTED]

In between the three hour reports, a slightly different strategy was used. As an example, suppose we wish to establish the [REDACTED] cloud cover at 18:00 on 5 June 2013. See Figure 8 below. The [REDACTED] station reports “Mainly Clear” at this time and at one hour previous and one hour later. The [REDACTED] and [REDACTED] stations both report “Mainly Clear” one hour previous and two hours later. We conclude then that the [REDACTED] site would have been “Mainly Clear” also at 18:00. Temperature was 16.1° and the wind was 6 m/s from a direction of 220°.

Time	T	deg	v	cloud cover	T	deg	v	cloud cover	T	deg	v	cloud cover	T	deg	v	cloud cover
21:00	12.4	320	7	-----	11.6	280	19	Mainly Clear	9.3	260	2	-----	13.0	280	15	-----
22:00	11.9	290	7	-----	11.5	270	24	Clear	8.2	240	5	-----	12.2	280	18	-----
23:00	11.3	290	9	-----	11.4	290	22	Clear	9.4	250	10	Clear	11.1	280	18	Clear
05-Jun-2013																
00:00	10.7	270	13	-----	10.9	280	26	Clear	9.5	240	12	-----	10.0	260	16	-----
01:00	11.0	270	19	-----	10.3	280	17	Clear	9.1	250	11	-----	9.8	270	20	-----
02:00	10.7	300	19	-----	9.6	290	13	Clear	9.1	250	10	-----	9.2	260	19	Clear
03:00	10.4	290	17	-----	8.7	280	11	Clear	8.5	260	12	-----	8.7	240	15	-----
04:00	9.9	310	17	-----	8.4	290	13	Clear	9.7	260	18	-----	7.7	230	19	-----
05:00	10.3	310	20	-----	7.8	270	13	Clear	8.9	270	13	Mainly Clear	7.0	230	13	Clear
06:00	11.0	310	20	-----	8.7	280	15	Clear	10.5	290	18	-----	8.5	240	17	-----
07:00	11.8	300	22	-----	10.1	300	20	Clear	11.5	310	21	-----	10.5	260	17	-----
08:00	12.5	320	22	-----	11.2	300	19	Mainly Clear	12.0	320	26	Mainly Clear	12.4	300	22	Clear
09:00	13.7	320	20	-----	11.6	280	20	Mostly Cloudy	12.6	320	22	-----	13.5	320	14	-----
10:00	14.1	320	22	-----	12.5	320	26	Mainly Clear	13.2	330	19	-----	14.0	250	16	-----
11:00	14.9	310	22	-----	13.2	310	15	Mainly Clear	13.8	350	19	Mainly Clear	15.1	250	20	Mostly Cloudy
12:00	14.5	330	19	-----	14.5	270	26	Clear	12.9	340	20	-----	15.5	270	17	-----
13:00	15.8	330	19	-----	15.4	300	19	Clear	13.7	350	17	-----	16.4	290	21	-----
14:00	16.2	300	13	-----	16.5	300	24	Clear	14.0	350	14	Mainly Clear	18.2	260	21	Mainly Clear
15:00	15.3	60	19	-----	17.8	290	26	Clear	14.5	10	15	-----	18.8	250	21	-----
16:00	15.9	60	17	-----	17.7	290	22	Mainly Clear	14.4	20	10	-----	19.4	270	22	-----
17:00	15.6	70	13	-----	17.4	270	22	Mainly Clear	14.3	50	9	Mainly Clear	17.9	250	19	Mainly Clear
18:00	16.1	220	6	-----	17.0	270	17	Mainly Clear	14.2	70	12	-----	18.5	250	24	-----
19:00	15.0	190	20	-----	15.9	300	13	Mainly Clear	13.3	100	6	-----	17.6	250	16	-----
20:00	13.8	200	20	-----	14.3	280	6	Mainly Clear	11.2	190	13	Mainly Clear	15.4	250	16	Mainly Clear
21:00	11.9	210	17	-----	9.4	260	7	Clear	10.7	160	20	-----	12.4	210	15	-----
22:00	11.6	230	17	-----	8.8	240	7	Clear	10.3	180	18	-----	11.3	240	10	-----
23:00	11.5	230	15	-----	9.1	250	11	Mainly Clear	10.7	220	11	Mainly Clear	10.3	210	13	Mostly Cloudy
06-Jun-2013																
00:00	11.0	260	11	-----	8.2	20	13	Clear	10.4	240	14	-----	9.6	240	15	-----

FIG. 8. Selection of weather data used to infer cloud cover at [REDACTED]

For most times, the cloud cover at the different stations was different or changing so that the above procedures did not yield an unambiguous result. Cloud cover at [REDACTED] could be established for approximately 11% of the hourly data available.

B. NRCan Meteorological Station

NRCan installed a meteorological tower at the HC2P measurement site, 2.5 km from the wind turbine identified as T2. Sensors to measure temperature, wind direction, wind speed (also humidity and pressure, but these were not used) were mounted at heights of 2 m and 10 m above the ground.²

Temperature was recorded every 60 s; wind was recorded every 5 s. The recorded times of day are Coordinated Universal Time (UTC). The measurements were saved in data files, each holding 24 hours of measurements. The files were uploaded daily to <ftp://ftp.seismo.nrcan.gc.ca/exports/HC/>. A folder labeled “w2” contains files of two types, one containing temperature (and humidity and pressure) data and one containing wind data

2013mmdd - THP-2m.txt

2013mmdd - WIND-2m.txt

and a folder labeled “w10” containing files

2013mmdd - THP-10m.txt

2013mmdd - WIND-10m.txt

² Heights of 2 m and 10 m have become the default and are what is readily available in standard instrumentation. Generally, having additional measurements at higher heights provides more accuracy.

The "mm" in the file names gives the month (00 to 12), the "dd" gives the day. These files were downloaded periodically to the MG Acoustics computers for analysis.

A sample of meteorological data (corrected) obtained on 22 August 2013 is shown in Figure 9 below. The top panel shows the temperature at the two heights. During the night, the temperature is greater at the 10 m height than at the 2 m height. During the day, as the ground warms up with the sun shining, these are reversed and the temperature at 10 m becomes less than that at 2 m. This is exactly what one would expect. The middle panel shows wind speed at the two heights. Clearly, the wind speed at 10 m is greater than that at 2 m. The bottom panel shows the wind direction. The measurement at the lower height shows more fluctuations; other days show similar behaviour.

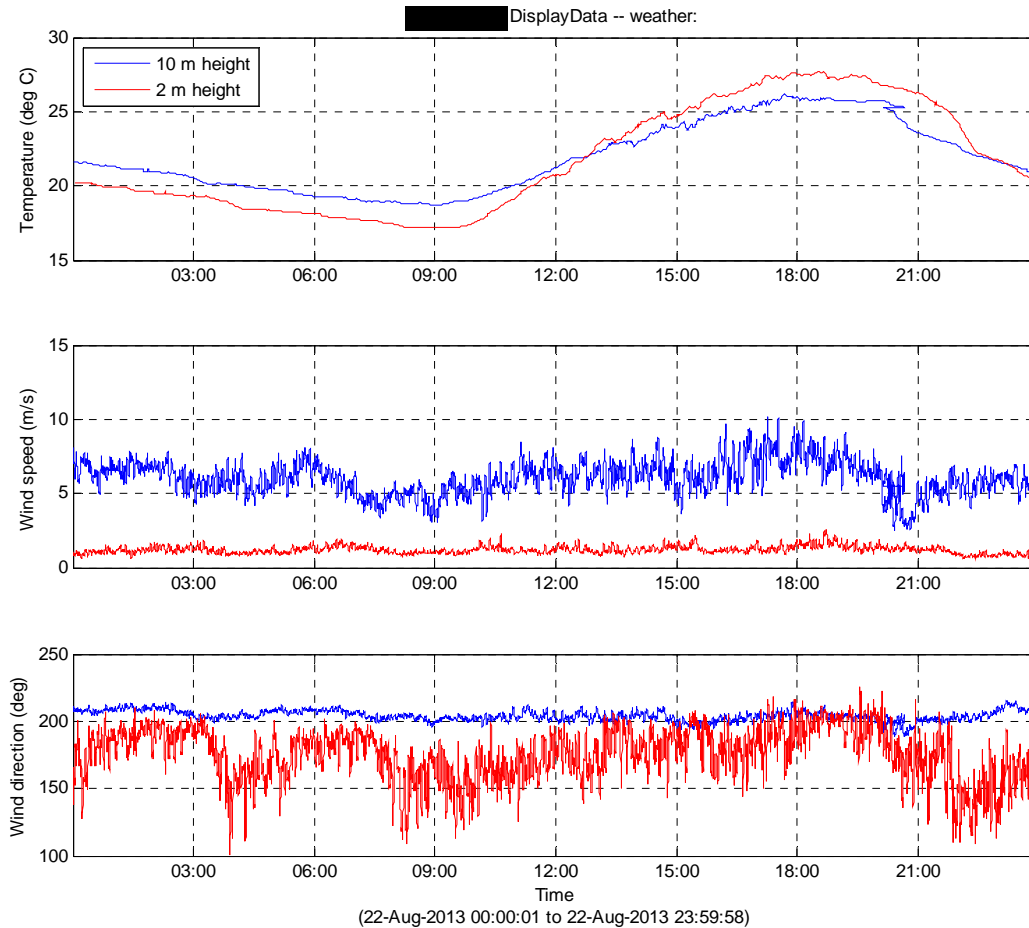


FIG. 9. Example of meteorological data collected

C. NRCan Acoustical Stations

The infrasound and low frequency sound data obtained at measurement stations HC1P, HC2P, HC3P and HC4P was uploaded daily to <ftp://ftp.seismo.nrcan.gc.ca/exports/HC/>. A folder labeled “HC1P” holds the data files, labelled as

2013mmdd.HC1P.HDF.M

where the "mm" in the file names gives the month and the "dd" gives the day. Data at the other three measurement stations was archived in similar fashion. These files were downloaded periodically to the MG Acoustics computers for analysis.

These data files are in ‘mini-Seed’ format, a format widely used by seismologists. Software to read these files into the Matlab environment was obtained at Matlab Central, a user file exchange site. Once installed, the low frequency sound pressure data and the parameters governing the data acquisition could be read into Matlab.

All sampling was done at 200 Hz, giving a bandwidth of 0 – 100 Hz. A calibration value (1/400,000) was provided by NRCan to convert from digital counts to instantaneous sound pressure in Pa. The recorded times of day are Coordinated Universal Time (UTC).

One example of sound pressure data downloaded is in Figure 10 below, showing the time-varying sound pressure signals as the blue traces for 23 June 2013. The panels, top to bottom, show the pressure at measurement stations HC1P, HC2P, HC3P and HC4P, respectively. The file from which this data was obtained contains 9335 contiguous records, each holding 4096 bytes of data, for each station.

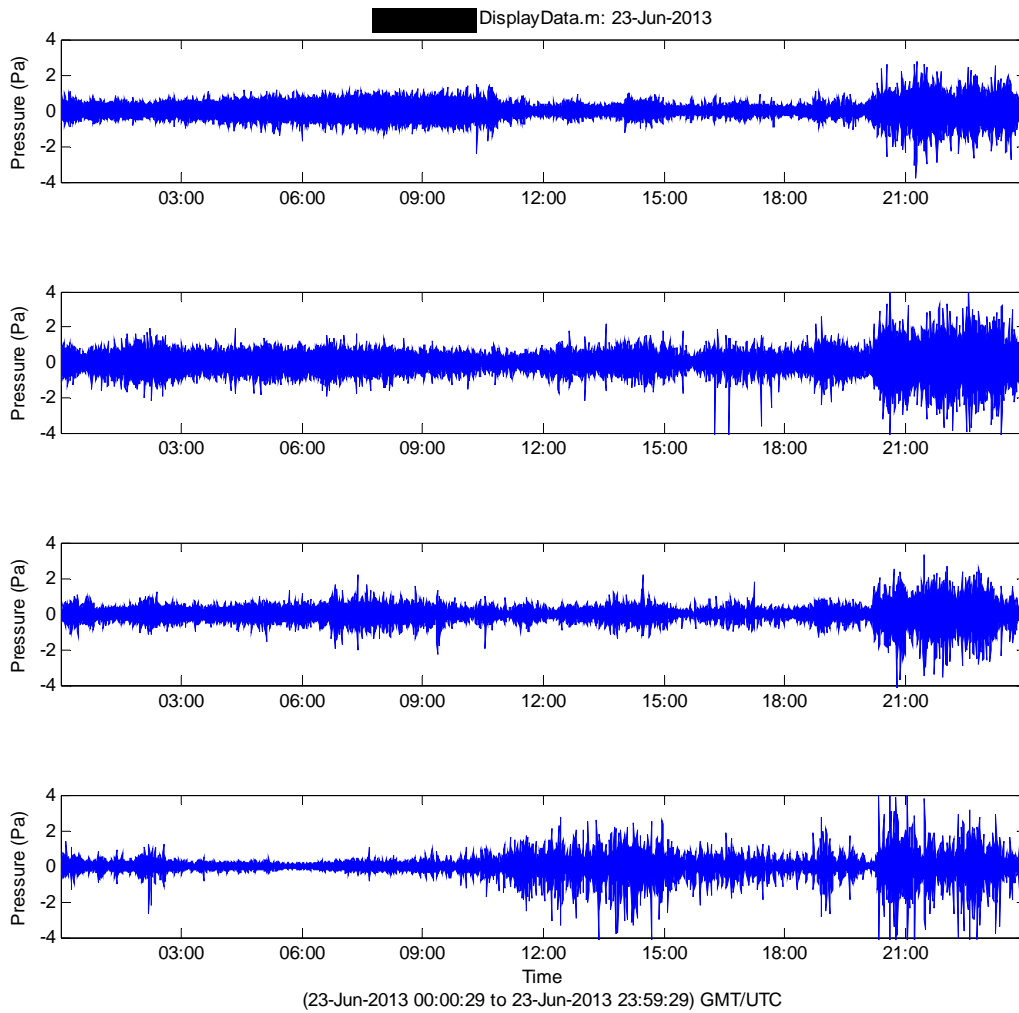


FIG. 10. Sample acoustic pressures obtained at the four measurement stations.

In the four traces shown here, it is not immediately apparent whether the acoustic signal are related to the wind turbine emissions, other sources of low frequency noise (e.g., factories or traffic), or natural ambient background levels (e.g., ocean wave motion). There does appear to be some correlation between the overall levels at the four sites.

To separate wind turbine noise from other sources, it is essential that the time histories be analyzed to get frequency response functions. We compute the power spectral density making use of Matlab's intrinsic functions. In particular, we use the "Welch" estimator with a "Hamming window". After some testing, it was found that a "SegmentLength" of 8192 with an "OverlapPercent" of 50 gave the best compromise between frequency resolution and noise reduction. All spectra computed have a frequency resolution of 0.0244 Hz. The size of data sample analyzed was typically one hour in length, but shorter samples of 10 minutes or 20 minutes were also used.

By way of example, the pressure signal at Station 1 (HC1P) shown in the top panel of Figure 10 has been analyzed hour by hour. The resulting 24 spectra are shown in Figure 11 below. All spectra show a rise of about 6 dB/octave as frequencies decrease. Much of this is assumed to be ambient background noise. In addition, the spectra contain well-defined peaks at frequencies of 0.8 Hz, 1.6 Hz, 2.4 Hz, etc. up to perhaps 6.4 Hz. Given that the blade passage frequency is expected to be 0.8 Hz, it seems very clear that these peaks can be ascribed to noise given off by the wind turbines.

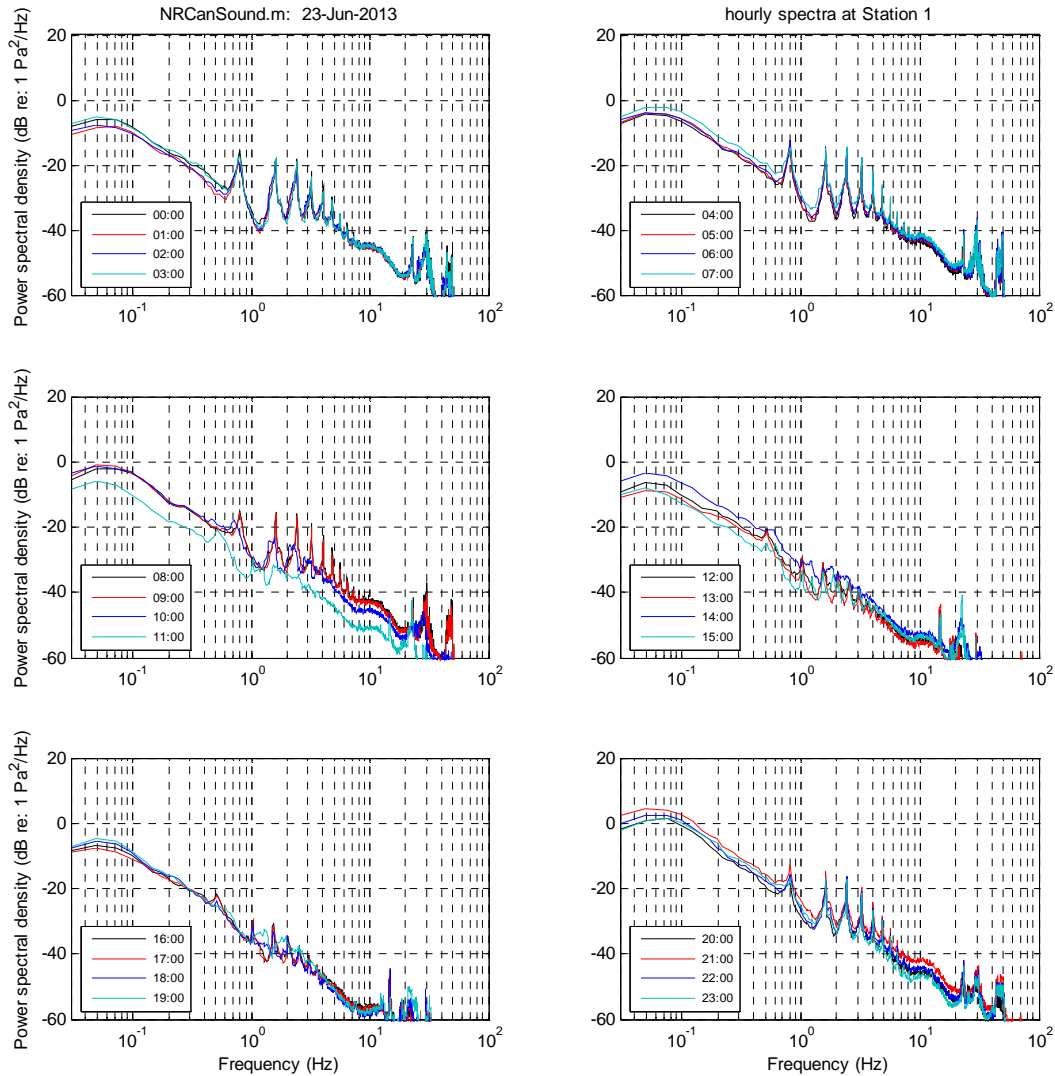


FIG. 11. Sample spectra computed for measurement station HC1P

Figure 12 shows the spectra obtained from the time traces for all four measurement stations.

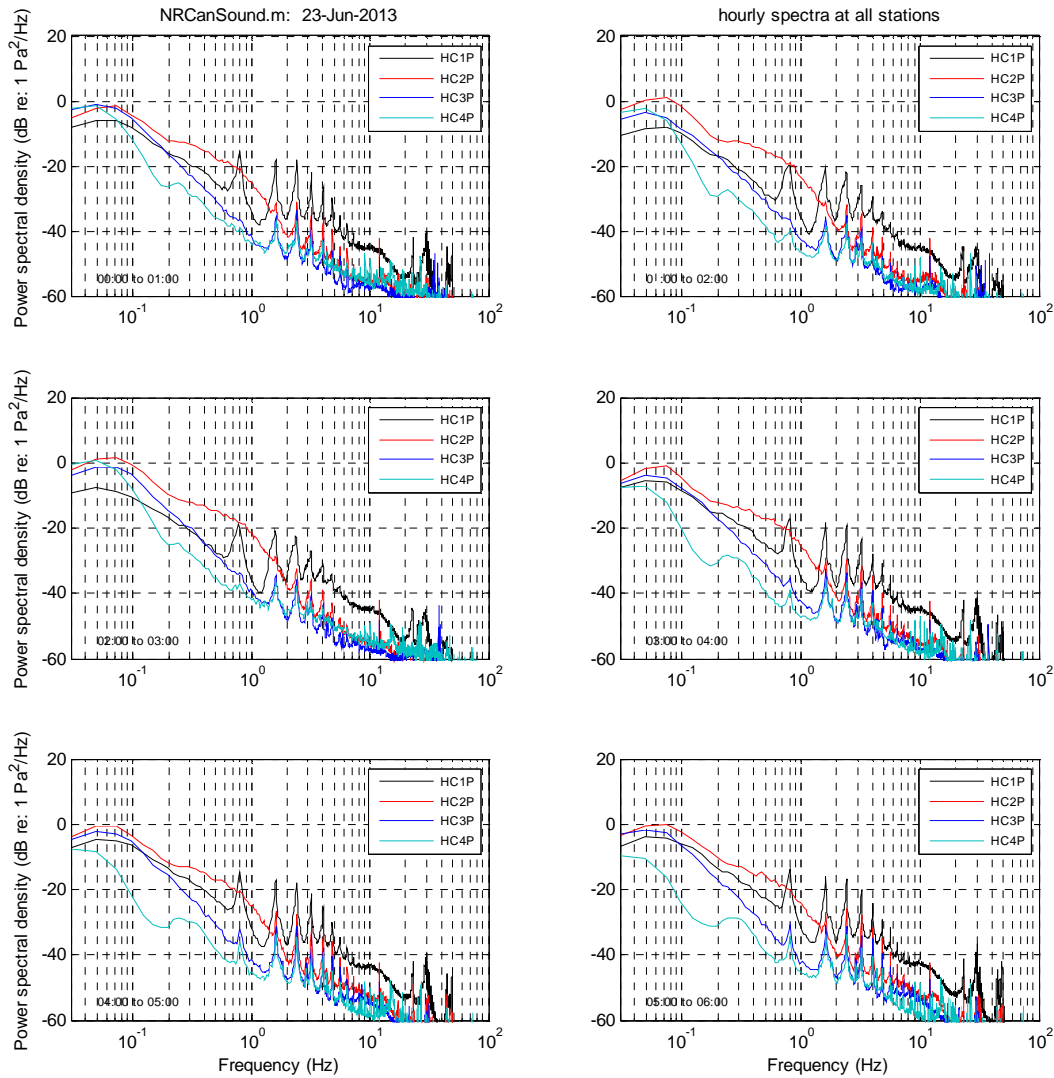


FIG. 12. Sample spectra obtained from the four measurement stations

Over the six hour period of these measurements, the skies were clear and the wind was fairly steady at about 19 km/hr. It is evident that the characteristic peaks at 0.8 Hz and its harmonics are present for all stations, including HC4P which is 10 km distant. This was not always possible; in fact, this example is quite a rare occurrence. Most often, the peaks are not evident in the spectra for HC4P.

D. [REDACTED] Wind Turbine Operational Logs

The operational logs for the four wind turbines were provided by the [REDACTED] for a few days of interest. Of particular interest is the log for 7-8 August 2013 during which time the wind turbines were cycled on and off at one hour spacing during daytime.

The logs were in the form of Excel data sheets. Readings for all four turbines were recorded every ten minutes. The time is local standard time, 4 hours behind UTC. The data recorded for each turbine were:

- ambient temperature
- ambient wind direction
- ambient wind speed
- rotor RPM
- blade pitch angle
- active power generation
- reactive power generation

The blade passage frequency is calculated from the rotor RPM. With three blades on each rotor, the blade passage frequency (in Hz) is 3/60 times the RPM.

E. Health Canada Data

A researcher from Health Canada made various independent sound pressure measurements at the [REDACTED] sites during the period of 27 July - 9 August 2013. Of particular interest are measurements made on 6-8 August 2013 at locations 125 m from wind turbine T2 at three different angular positions. These data allow us to assess the directionality of the noise emission from the turbine. The files for the three angular positions are labelled (by HC) [REDACTED] and [REDACTED] with these angles indicating the wind direction that would make the measurement location be downwind. So, if the wind is coming from the west (a wind direction of [REDACTED] the [REDACTED] measurement location would be nearly downwind of the tower T2.

The data for position [REDACTED] is in three files:

- 06-Aug-2013 09:33:21 - 06-Aug-2013 23:59:51
SR_130806 093321 2250 0.049414 125m 175degreeWind groundboard.wav
- 07-Aug-2013 00:00:01 -- 08-Aug-2013 00:00:01
SR_130807 000001 2250 0.049414 125m 175degreeWind groundboard.wav
- 08-Aug-2013 00:00:01 -- 09-Aug-2013 00:00:01
SR_130808 000001 2250 0.049414 125m 175degreeWind groundboard.wav

Data for position [REDACTED] is also in three files:

- 06-Aug-2013 11:03:19 - 07-Aug-2013 11:03:09
SR_130806 110319 2250 0.0501 125m 272degreeWind soaker.wav
- 07-Aug-2013 11:03:19 -- 08-Aug-2013 11:03:19
SR_130807 110319 2250 0.0501 125m 272degreeWind soaker.wav
- 08-Aug-2013 11:03:19 -- 09-Aug-2013 11:03:19
SR_130808 110319 2250 0.0501 125m 272degreeWind soaker.wav

Data for position [REDACTED]° is in four files:

- 06-Aug-2013 10:21:13 -- 07-Aug-2013 00:00:00
SR_130806 102113 2270 0.05042 125m 310degreeWind groundboard.wav

07-Aug-2013 00:00:01 -- 08-Aug-2013 00:00:01
SR_130807 000001 2270 0.05042 125m 310degreeWind groundboard.wav
08-Aug-2013 00:00:01 -- 08-Aug-2013 08:48:01
SR_130808 000001 2270 0.05042 125m 310degreeWind groundboard.wav

The start and end times, indicated in the file name, are local time, i.e., Atlantic Daylight time, 3 hours behind UTC. These are wav files that can be imported directly into Matlab for analysis. Sampling was at 8000 Hz/24 bit. The data was downsampled to 200 Hz then power spectra computed, as explained in Section III.C., using data frames of 10 minutes or 20 minutes duration.

Health Canada also set up a meteorological station near NRCan station HC1P. Readings of wind and temperature at heights of 2 m and 10 m were made every second over a four day period. The file “WStn1_20130805_20130809_SS_██████████.csv” contains the data. The desired quantities were averaged over 10 minutes or 20 minutes, consistent with the selection of data frame size for the power spectral analysis.

It is noted that the ██████████ was cycling their wind turbines on and off during August 7 and 8.

Analysis of these measurements is shown in Section VII.D.

V. MODELS OF METEOROLOGICAL AND SOUND SPEED PROFILES

A. Similarity Scaling

1.) The equations

The variation of sound speed with height is dependent on the variations of both wind speed and temperature with height. Measurements by many research groups have shown that temperature and wind speed profiles can be approximated by characteristic functions known as similarity equations. There is considerable scatter in the data on which the equations are based, though – hence, considerable uncertainty must be anticipated in any predictions of sound speed profiles based on these equations.

Shown below are the traditional functions used by MG Acoustics in the analysis of meteorological data taken during acoustic propagation measurements. These similarity equations are appropriate for heights up to one-tenth the boundary layer height, so 100-200 m or so.

The wind speed $u(z)$ varies with height z according to the relation

$$u(z) = \frac{u_*}{\kappa_a} \left[\ln \left(\frac{z}{z_o} \right) - \psi \left(\frac{z}{L} \right) \right] , \quad z > z_o , \quad (1)$$

where u_* is a wind speed scaling parameter called the friction velocity, κ_a is the von Karman constant (taken as 0.4), z_o is the surface roughness, L is the Monin-Obukhov length, and the function ψ is

$$\psi \left(\frac{z}{L} \right) = \begin{cases} \ln \left[\left(\frac{1+x^2}{2} \right) \left(\frac{1+x}{2} \right)^2 \right] - 2 \arctan x + \frac{\pi}{2} & , \frac{z}{L} < 0 \\ -5 \frac{z}{L} & , \frac{z}{L} > 0 \end{cases} \quad (2)$$

with

$$x = \left(1 - 16 \frac{z}{L} \right)^{1/4} . \quad (3)$$

If the wind speed is measured at a height z_w , then the measured value is

$$u_w = \frac{u_*}{\kappa_a} \left[\ln \left(\frac{z_w}{z_o} \right) - \psi \left(\frac{z_w}{L} \right) \right] , \quad (4)$$

The temperature profile is given by

$$T(z) = T_1 + \frac{T_*}{\kappa_a} \left[\ln \left(\frac{z}{z_1} \right) - \psi_h \left(\frac{z}{L} \right) + \psi_h \left(\frac{z_1}{L} \right) \right], \quad (5)$$

where T_* is the temperature scaling parameter and the function ψ_h is given by

$$\psi_h \left(\frac{z}{L} \right) = \begin{cases} 2 \ln \left[\frac{1}{2} \left(1 + \sqrt{1 - 16 \frac{z}{L}} \right) \right] & , \frac{z}{L} < 0 \\ -5 \frac{z}{L} & , \frac{z}{L} > 0 \end{cases} . \quad (6)$$

The temperature T_1 is a reference temperature measured at a height z_1 . To apply the equations of similarity, it is necessary to have a second temperature T_2 measured at a different height z_2 . This height should be higher, i.e., $z_2 > z_1$. Taking the difference in temperatures:

$$\Delta T = T_2 - T_1 = \frac{T_*}{\kappa_a} \left[\ln \left(\frac{z_2}{z_1} \right) - \psi_h \left(\frac{z_2}{L} \right) + \psi_h \left(\frac{z_1}{L} \right) \right]. \quad (7)$$

In the two equations 4 and 7, there are three unknowns: L , T_* , and u_* . A solution is made possible by including a third, general relation:

$$L = \frac{T_s}{\kappa_a g} \frac{u_*^2}{T_*}, \quad (8)$$

where g is the acceleration of gravity (9.81 m/s^2) and T_s is a “surface temperature”. We have used a value of $T_s=290 \text{ K}$ in our analyses.

2. Converting measured temperatures and wind speed to vertical profiles

The measured data is the temperature difference ΔT and the wind speed u_w . These are used to compute the vertical wind and temperature profiles.

(a) Test for similarity

The first step is to check that the equations of similarity are applicable. The following relation is a necessary condition for the equations to have a solution:

$$u_w^2 > \frac{5 g z_w^2}{T_s (z_2 - z_1)} \Delta T \quad (9)$$

If this relation is true, then the equations of similarity can be used. This will always be the case during “lapse” conditions, when ΔT is negative, and rays are propagated upwards. It will also hold during “inversion” conditions provided the wind speed is sufficiently large. It is recommended that heights of $z_w = z_2 = 10$ m and $z_1 = 2$ m be used for measurements. In MKS units, the test relation is approximately

$$u_w^2 > 2\Delta T . \quad (10)$$

(b) Profiles when similarity holds

If Eq (9) holds, then similarity is applicable. The calculation is as follows.

First, the unknown parameters u_* , T_* , and L must be determined from the measured values, ΔT and u_w . It is necessary to use an iterative procedure:

1. assume an initial huge value of $L=1 \times 10^{10}$
2. calculate z_1/L , z_2/L , and z_w/L
3. from Eq (4) using measured u_w , calculate u_*
4. from Eq (7) using measured ΔT , calculate T_*
5. compute new value of L using Eq (8)
6. go back to step 2.

After 10 iterations, the procedure will have converged very accurately. The values of L , u_* , and T_* at the end of the procedure are the final solutions. They are then used within Eq (1) to calculate the wind speed profile at all desired heights z and within Eq (5) to calculate the temperature profile at all desired heights.

An example is shown below in Figure 13. For 14 July 2013 at 16:00, it was found that the temperatures at 2 m and 10 m height were 29.5 and 29.8, respectively, and the wind speed at 10 m height was 1.96 m/s. With this information, the above procedure is used and temperature and wind speed profiles determined. The wind speed at 2 m height obtained from the profile is 0.93 m/s; this agrees fairly well with the actual wind speed of 1.01 m/s.

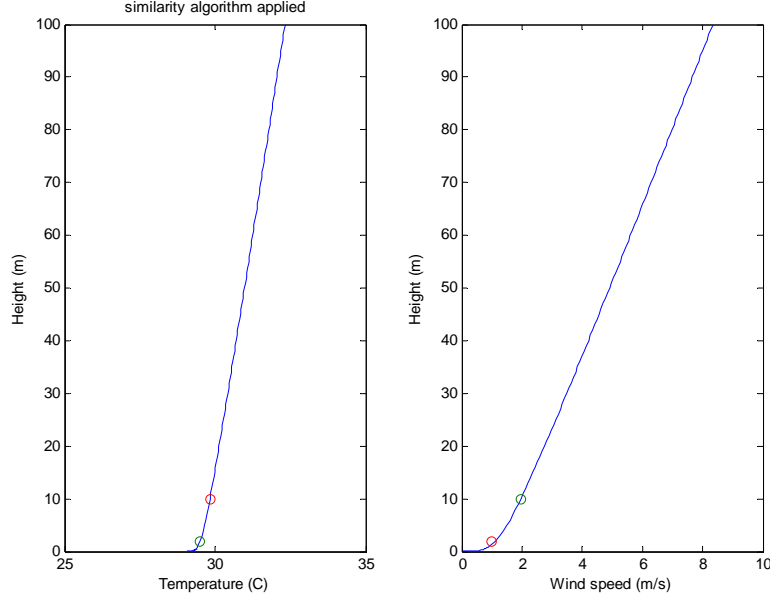


FIG. 13. Temperature and wind speed profiles computed using similarity

(c) Profiles when similarity does not hold

If the relation in Eq (10) is not true, then similarity is not applicable. Logarithmic profiles are assumed for both temperature and wind speed. The following formulae may be used:

$$u(z) = u_w \frac{\ln(z/z_o)}{\ln(z_w/z_o)} \quad (11)$$

and

$$T(z) = T_1 + (T_2 - T_1) \frac{\ln(z/z_1)}{\ln(z_2/z_1)} \quad (12)$$

(d) Sound speed profile from similarity scaling functions

The sound speed profile is obtained from the following equation,

$$c(z) = c_0 + \left(\frac{1}{2} \frac{c_0}{T_0} \right) T(z) + u(z) \cos(u_{\text{prop}} - u_{\text{dir}}) \quad (13)$$

where $c_0 = 331.4$ m/s is the reference sound speed, $T_0 = 273$ K is the reference temperature, u_{prop} is the direction of propagation, u_{dir} is the direction of the wind, and the temperature $T(z)$ is specified in °C.

As a general rule of thumb, the sound profile must be known to about 1/10 the propagation distance (admittedly, this rule has not been well tested). However, similarity is only generally valid up to 1/10 of the boundary layer thickness (500 m to 2000 m). Therefore caution is required when using similarity for propagation distance greater than about 2 km. For larger propagation distances (> 2 km), it is best to use data obtained from weather balloons, radar, sodar, etc.

B. Sound speed Profile from Weather Classes

The approach described in the previous section required measurements of wind speed at 10 m height and temperature at heights of 2 m and 10 m. There may be occasions when such meteorological measurements are not possible. Some other approach is needed.

We consider here an alternate approach that makes use of weather data, as reported by Environment Canada for example. Knowing the temperature and wind at a single height and the cloud cover, it is possible to assign wind and stability classes and, from these, to generate a sound speed profile.

In recent years, approximate procedures have been developed to obtain the sound speed profile from general meteorological observations. It has been found (references [4] and [5]) that the sound speed profile can be approximated by the following equation³,

$$c(z) = c(0) + B \ln\left(\frac{z}{z_0} + 1\right) + Az \quad , \quad (14)$$

where the coefficients A and B are obtained from different versions of the similarity functions. The term $c(0)$ is nominally the speed of sound at ground level, typically taken as 340 m/s. It is not necessary to have an exact value for this constant term because the sound propagation models respond to the variation of sound speed with height. In our comparison of this weather class approach to the similarity approach, we have made the sound speeds at ground level to be the same in both approaches.

During the day (stability classes S_1 , S_2 and S_3),

$$A = \frac{u_* \cos(u_{\text{prop}} - u_{\text{dir}})}{\kappa_a L} + \left(\frac{1}{2} \frac{c_0}{T_0}\right) \left(0.74 \frac{T_*}{\kappa_a L} - \frac{g}{c_p}\right) \quad (15a)$$

during the night (stability classes S_4 and S_5 ,

³ Most, but not all, reports originating from the Nord2000 and Harmonoise projects use this expression. In the exceptions (e.g., [6]), the "1" in the logarithm term is dropped. The difference introduced is negligible and corresponds to a shift of the origin of z , by z_0 .

$$A = 4.7 \frac{u_* \cos(u_{\text{prop}} - u_{\text{dir}})}{\kappa_a L} + \left(\frac{1}{2} \frac{c_0}{T_0} \right) \left(4.7 \frac{T_*}{\kappa_a L} - \frac{g}{c_p} \right) \quad (15b)$$

and

$$B = \frac{u_* \cos(u_{\text{prop}} - u_{\text{dir}})}{\kappa_a} + \left(\frac{1}{2} \frac{c_0}{T_0} \right) \left(0.74 \frac{T_*}{\kappa_a} \right) \quad (16)$$

where $c_p = 1005 \text{ J/kg K}$ is the specific heat capacity of air at constant pressure.

The wind speed and the atmospheric stability are assigned classes according to Tables 3 and 4. The meteorological parameters u_* and T_* and the inverse of the Monin-Obukhov length $1/L$ are obtained from the wind speed and stability classes according to Tables 5, 6, and 7.

TABLE 3. Wind speed classification

wind speed component at 10 m above ground	wind speed class
0 to 1 m/s	W1
1 to 3 m/s	W2
3 to 6 m/s	W3
6 to 10 m/s	W4
> 10 m/s	W5

TABLE 4. Classification of atmospheric stability

time of day	cloud cover	stability class
day	0/8 to 2/8	S1
day	3/8 to 5/8	S2
day	6/8 to 8/8	S3
night	5/8 to 8/8	S4
night	0/8 to 4/8	S5

TABLE 5. Friction velocity, by wind speed class

wind speed class	u_* in m/s
W1	0.00
W2	0.13
W3	0.30
W4	0.53
W5	0.87

TABLE 6. Temperature scale T^* , by wind class and stability class

	S1	S2	S3	S4	S5
W1	-0.4	-0.2	0.0	+0.2	+0.4
W2	-0.2	-0.1	0.0	+0.1	+0.2
W3	-0.1	-0.05	0.0	+0.05	+0.1
W4	-0.05	0.0	0.0	0.0	+0.05
W5	0.0	0.0	0.0	0.0	0.0

TABLE 7. Inverse of the Monin-Obukhov length $1/L$, by wind speed class and stability class

	S1	S2	S3	S4	S5
W1	-0.08	-0.05	0.0	+0.04	+0.06
W2	-0.05	-0.02	0.0	+0.02	+0.04
W3	-0.02	-0.01	0.0	+0.01	+0.02
W4	-0.01	0.0	0.0	0.0	+0.01
W5	0.0	0.0	0.0	0.0	0.0

Note that the stability class cannot be calculated using the data collected by the NRCan measurement stations since this data does not include cloud cover information.

VI. COMPARISON OF COMPUTED SOUND SPEED PROFILES

There is interest in seeing if Environment Canada weather data can be used to assign weather classes and hence determine sound speed profiles. This could be useful when a dedicated weather station is unavailable and sound speed profiles are required for an acoustical propagation calculation. The method of using Environment Canada data to generate profiles was described in Section V.B. To test this procedure, we will compare against sound speed profiles generated using data from the dedicated NRCan weather station at HC2P using the established similarity method of Section V.A.

First, the data accumulated from the Environment Canada website archives was screened and sorted, to determine the occurrence of specific stability and wind classes. There is an immediate challenge to equate the Environment Canada definitions of cloud cover with the Harmonoise/Nord2000 definitions discussed in the previous Section. The following correspondence table was used:

TABLE 8. Correspondence table, to relate Environment Canada observations to Harmonoise stability classes

Environment Canada		Harmonoise stability class	
classification	cloud cover	day	night
Clear	0/10	S1	S5
Mainly Clear	1/10 - 4/10	S1 or S2	S5
Mostly Cloudy	5/10 - 9/10	S2 or S3	S4
Cloudy	10/10	S3	S4

There was no unambiguous way of identifying a S2 stability class because its definition (3/8 - 5/8 cloud cover) straddles the “Mainly Clear” and “Mostly Cloudy” classifiers.

After sorting through the Environment Canada, examples of most of the Harmonoise/Nord2000 stability and wind classes were identified. No high-wind W5 conditions were found, though, and no low-wind W1 conditions were found during the day.

Given the stability and weather class at a particular hour, the temperature, wind, and sound speed profiles can be determined, as described in Section V.B. For the same hour, data from the NRCan meteorological station (mean temperatures at 2 m and 10 m heights, wind speed at 10 m height) can be used to generate an alternate set of profiles.

In the following, examples of specific conditions will be selected and the two approaches compared. Given that the number of combinations of wind class, stability class and wind direction is large, only a representative selection of examples is presented.

On 3 October at 15:00 local standard time, Environment Canada web archives report that wind was from 300° with a speed of 8.3 m/s at the [REDACTED] weather station. Using cloud cover information from weather stations at [REDACTED], [REDACTED] and [REDACTED], we find that the cloud cover at [REDACTED] was most likely “Clear” or “Mainly Clear”. Therefore, the stability

class is either S1 or S2 and the wind class is W4. With the reported temperature of 18.8° at 10 m height, the equations of Section V.B. are used to compute temperature profiles and wind speed profiles for both S1 and S2 classes. These are shown in Figure 14 as the two solid curves in the left and middle panels. Both stability classes give similar temperature profile: this is a lapse condition that will cause sound rays to diffract upwards in the absence of wind (crosswind for example). The wind speed profiles are significantly different. That computed for class S1, with wind speed decreasing with height above 100 m, is decidedly unrealistic. This confirms the expectation that the Harmonoise/Nord2000 scheme is not intended to produce realistic profiles above 100-200 m height.

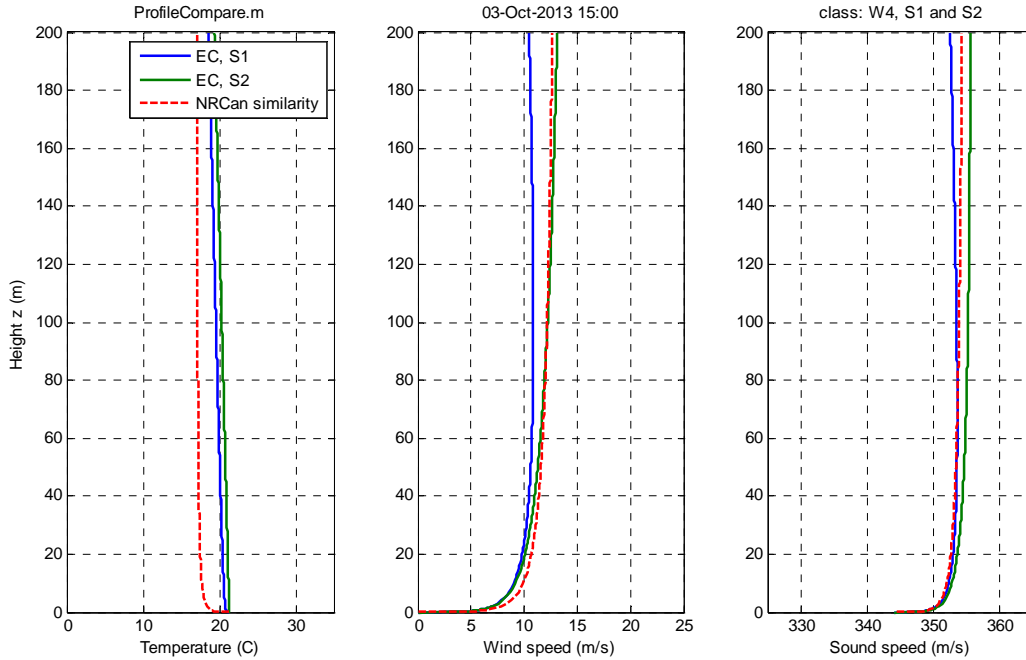


FIG. 14. Comparison of temperature, wind speed and sound speed profiles obtained using similarity and a weather class approach

The propagation direction is 285° . Thus, with a wind coming from 300° , we have downwind propagation. The sound speed profiles computed for the two stability classes are shown in the right panel of this figure. Agreement is good up to 100 m height, above which the difference between the two becomes progressively evident as height increases.

The alternate approach (and the one we consider to be more rigorous) is to use meteorological data obtained by the NRCan met station at HC2P and apply the equations of similarity, as described in Section V.A. From this data (at 19:00 UTC), we find a wind speed of 9.9 m/s at 10 m height, and temperatures of 17.7° and 18.4° at heights of 2 m and 10 m, respectively. These produce the temperature, wind speed and sound speed profiles shown as the dashed curves in the above figure. The temperature profile is quite different from those obtained using the weather class approach. The lapse is not nearly so severe at the larger heights. The wind speed profile is closer to that for the S2 class than the S1 class. In the end, though, the errors introduced by the weather class approach in the temperature profile and the wind speed profile tend to cancel when the sound speed profile is computed for this downwind case.

For the next example, we select 1 August at 00:00 local standard time. From the Environment Canada information, we have stability class S5 and wind class W3; wind is from 230°. The NRCan data gives a wind speed of 4.8 m/s and temperatures of 16.85° and 18.3° at 2 m and 10 m heights, respectively. Comparing temperature and wind speed profiles, in Figure 15, we see that the two approaches give quite different results. This carries over to the sound speed profiles. The similarity approach with NRCan data gives a profile that is more strongly downward refracting.

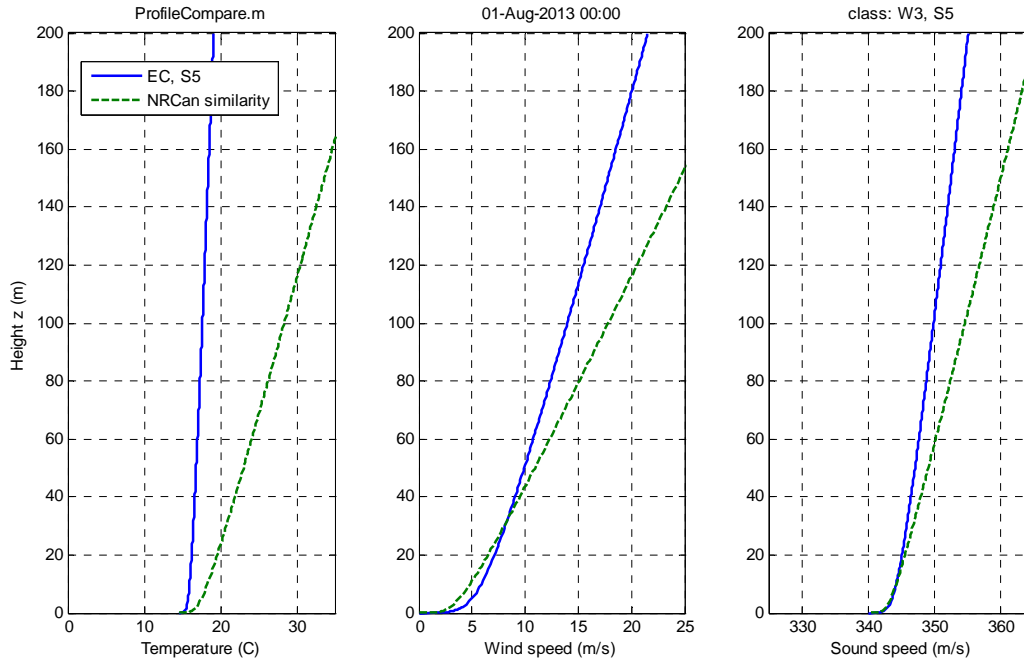


FIG. 15. Comparison of temperature, wind speed and sound speed profiles obtained using similarity and a weather class approach

The next example, in Figure 16, was for a “Cloudy” day, on 11 June 2013 at 13:00 local standard time. From the Environment Canada data we have a wind class W3 and stability class S3, with the wind from 230°. The NRCan sensors reported the same temperature 16.85° at both 2 m and 10 m height and a wind of 5.12 m/s coming from 230°. The wind speed profiles are in nearly perfect agreement. The difference between the two sound speed profiles is mainly the difference in wind direction -- the NRCan wind direction is almost perpendicular to the propagation direction so the cosine term in the formula reduces the wind contribution to a smaller amount than is calculated for the Environment Canada data.

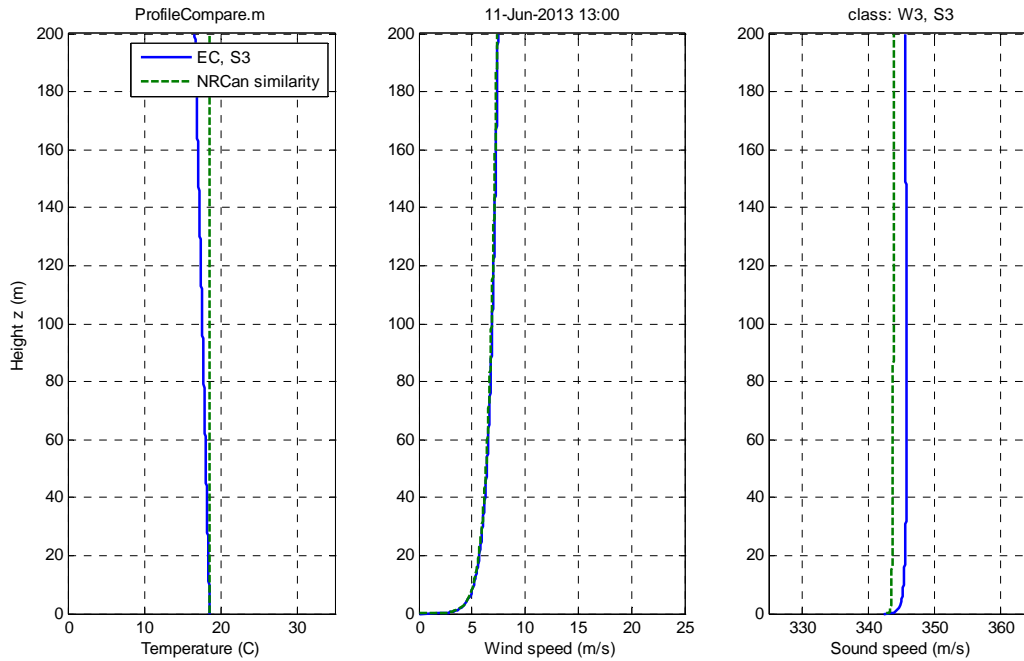


FIG. 16. Comparison of temperature, wind speed and sound speed profiles obtained using similarity and a weather class approach

An example for a cloudy night is shown in Figure 17, for 8 July 2013 at 04:00. The Environment Canada data makes the wind class W2 and the stability class S4. With the wind from XXXX°, propagation is mostly downwind. Both temperature and wind speed profiles are quite different than those computed using similarity and the NRCan data. The resulting sound speed profile from NRCan similarity is almost constant with height once above 20 m. The Environment Canada data shows downward refraction.

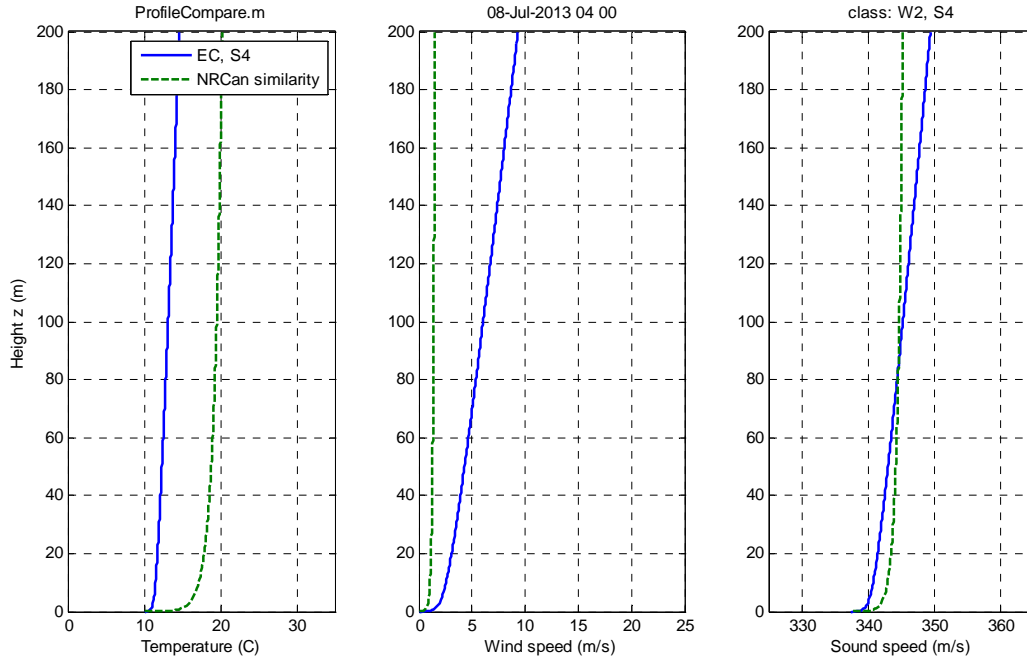


FIG. 17. Comparison of temperature, wind speed and sound speed profiles obtained using similarity and a weather class approach

The next example demonstrates how wrong the weather class approach can get. Environment Canada data for 14 July at 16:00 local standard gives a wind class of W2 and a stability class of S1 or S2. The resulting temperature and wind speed profiles for these classes are very different from those calculated from the NRCan data using similarity, as evident in Figure 18 below. We show the profiles up to 1000 m for this example. It is especially disconcerting that the wind speed for S1 becomes negative above 200 m height and for S2 becomes negative above 500 m height. These results are clearly unphysical. The wind, at 180° , is nearly downwind. Downward refracting sound speed profiles are anticipated but the weather class approach gives a slightly upward refracting profile.

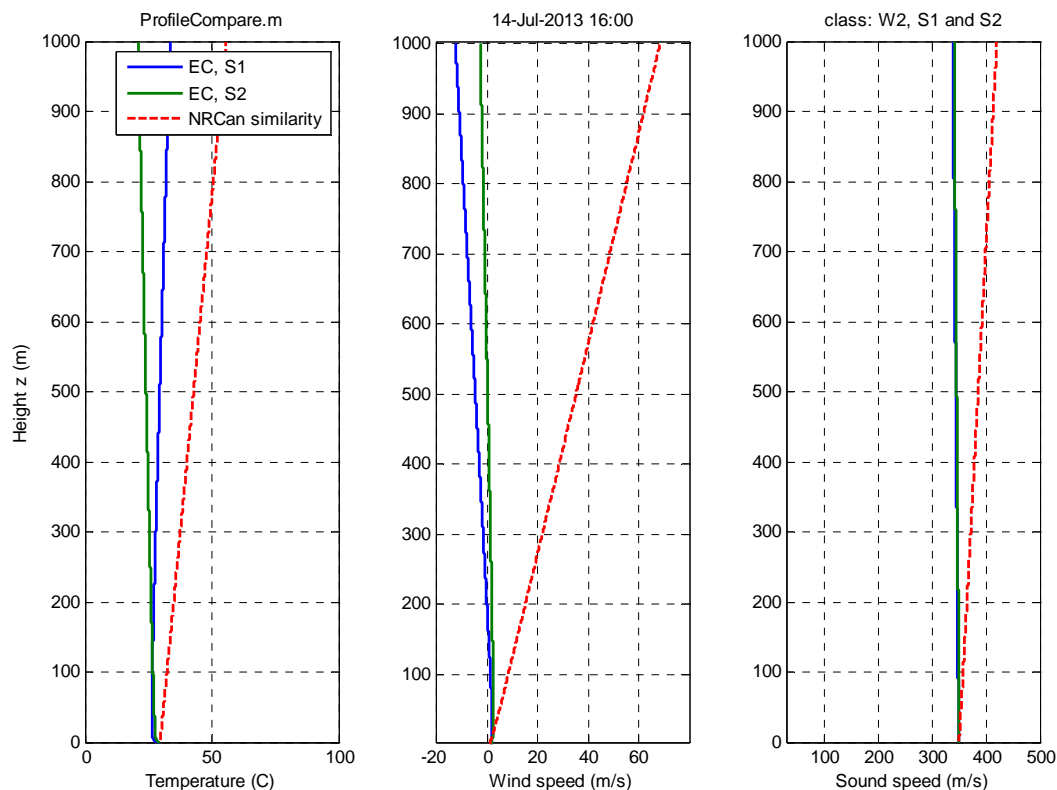


FIG. 18. Comparison of temperature, wind speed and sound speed profiles obtained using similarity and a weather class approach

As another example, shown in Figure 19, we consider observations for 9 October at 05:00. Environment Canada weather information gives a wind class of W2 and a stability class of S5. Wind is ████, in the propagation direction. The equations of Section V.B. lead to profiles that are strongly downward refracting. By comparison, the use of similarity with the NRCan meteorological data gives profiles that are not so strongly downward refracting -- both temperature and wind speed profiles are logarithmic with height.

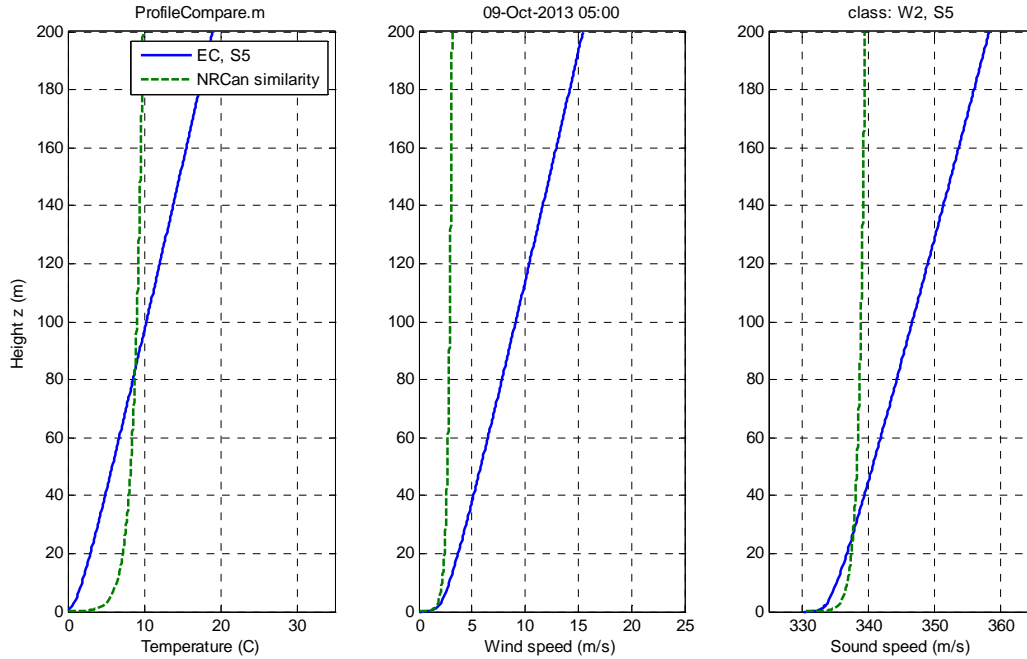


FIG. 19. Comparison of temperature, wind speed and sound speed profiles obtained using similarity and a weather class approach

Finally, in Figure 20, we consider an upwind propagation example. For 9 July at 01:00, we find from the Environment Canada weather information that we have a wind class W2 with a stability class S5. The wind direction is ██████, nearly directly upwind. The resulting temperature profile shows a strong lapse, i.e., it will cause sound to refract downward. The use of similarity with NRCan meteorological data gives a logarithmic profile having much less downward refraction of sound. The wind speed, using the weather class approach, varies greatly with height, unlike the similarity calculation. With upwind propagation, this would give strong upward refraction. Thus, we have temperature with strong downward refraction being balanced by wind speed with strong upward refraction. The resulting sound speed profile shows just a slight upward refraction. By comparison, the similarity approach shows a slight downward refraction. Over the first 100 - 200 m of height, the two approaches are, by good fortune, somewhat similar.

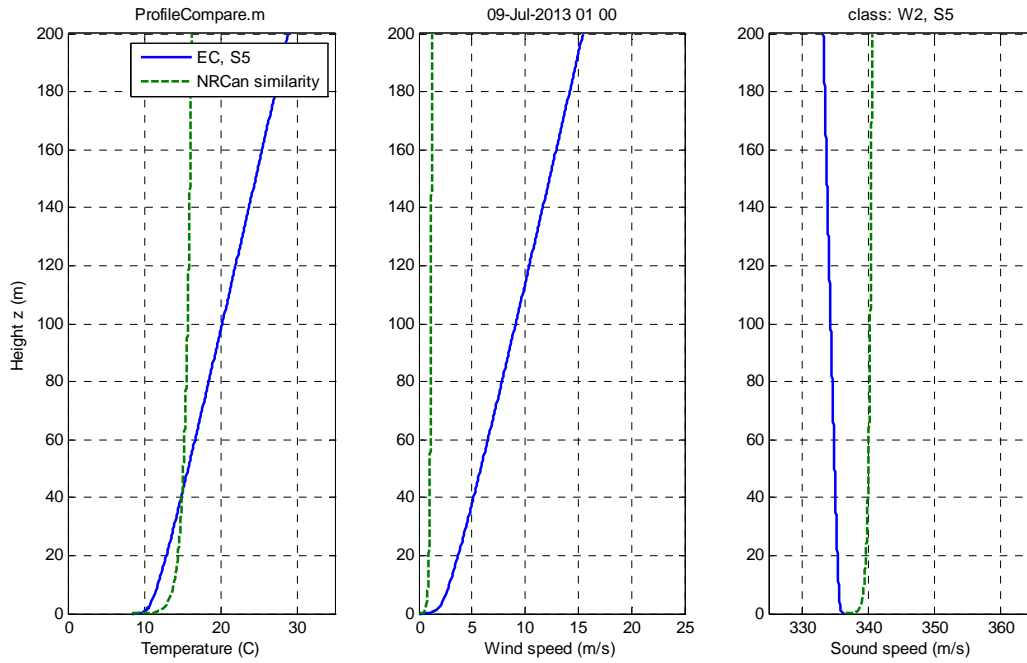


FIG. 20. Comparison of temperature, wind speed and sound speed profiles obtained using similarity and a weather class approach

VII. WIND TURBINE CYCLING TEST

On 7 August and 8 August, the operators of the [REDACTED] wind turbines cycled the four turbines on and off during the daytime. This was critically important as it allows us to separate the wind turbine noise from other sources of noise. Additionally, Health Canada had instrumentation set up around wind turbine T2 during this time, enabling us to assess the radiation and directivity of this turbine.

A. Experiment Overview

Figure 21 below summarizes the experimental situation. The continuous curves in the top panel plot the wind speed measured by sensors in the four wind turbines (T1, T2, T3, and T4) and the circles indicate the hourly wind speed reported by Environment Canada. The middle panel shows the blade passage frequency of the four turbines, as obtained from their operational logs. The bottom panel shows the sound pressure time history measured at station HC1P.

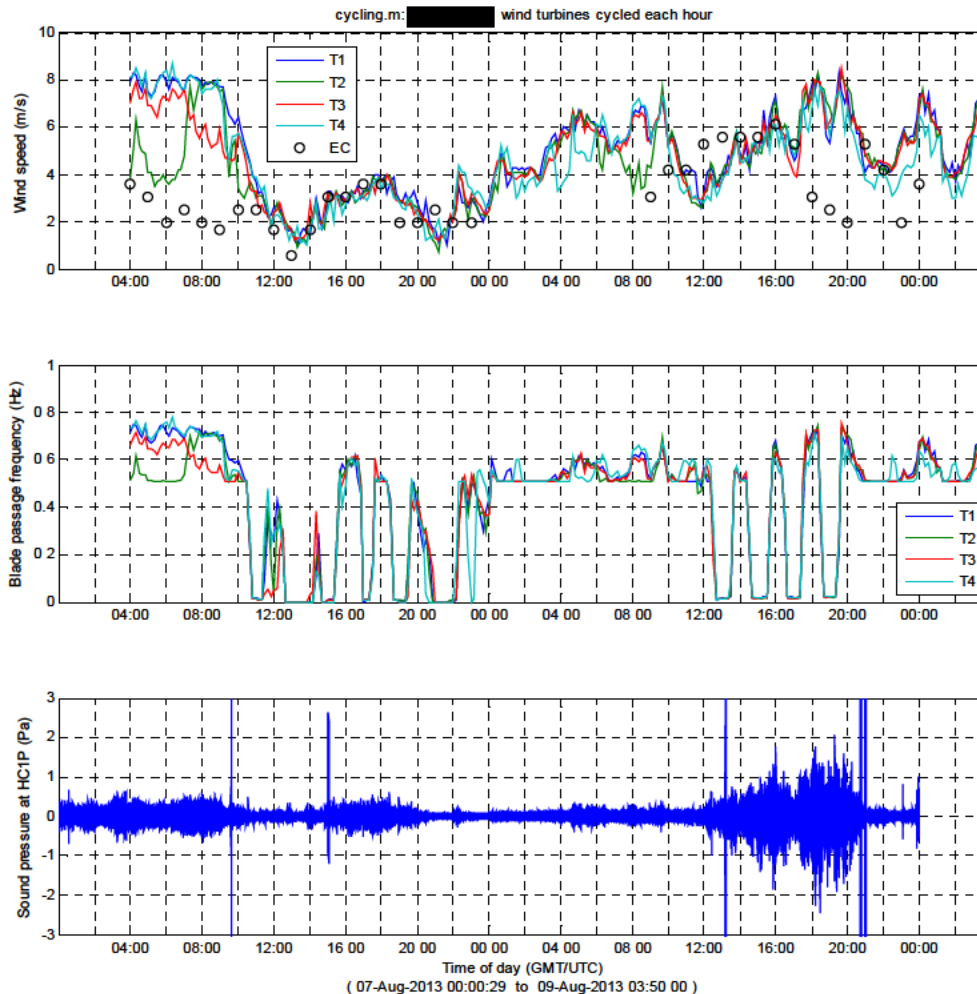


FIG. 21. Wind turbine cycling test

The wind speeds reported for the four wind turbines are closely correlated. There are some differences but, given that there is considerable distance between some of the turbines (T1 and T3 are separated by 910 m), this is not unexpected. There is a bigger difference between the wind turbine speeds and the wind speed reported by Environment Canada, although there is fairly good correlation. We presume that these are due to the different sensor heights – the wind turbine sensors are at a height of 80 m, those for Environment Canada are at 10 m.

The blade passage frequencies of the four wind turbines are closely correlated with each other and with the wind speed that they are sensing. During normal operation, when the wind speed drops below about 5 m/s, the turbine goes into an "idling" mode in which the blade passage frequency is kept at about 0.5 Hz and no power is generated. This is clearly evident at times during the night. The cycling of the wind turbines during the daytime was not normal as the operators forced the blades to completely stop turning during the "off" times⁴ and did not enforce the idling criterion during the "on" times.

The sound pressure signal seems to correlate with the wind speed somewhat. We need to examine the spectral information to see this more clearly.

B. Spectral Comparisons

From the blade passage frequency plot of the previous figure, the "on" and "off" intervals of the wind turbines are clearly evident. We can pull out measured sound pressure time histories during these intervals and determine the power spectra.

The next series of four figures presents the results. Figure 22 shows the first five intervals on 7 August (on, off, on, off, on); Figure 23 shows the next five intervals (on, off, on, off, on) on this day, with the interval from 15:45 – 16:45 common to both. Figures 24 and 25 show the cycling on 8 August.

Stepping through the cycles on both days, there are a couple general observations.

First, the overall level of the spectra increases with wind speed. This observation holds whether the wind turbines are on or off. The noise generated by the wind turbines and the noise due to other sources (natural or otherwise) both tend to increase with wind speed. The overall shapes of the spectra are also similar whether the turbines are on or off.

Second, the overall level of the spectra does seem to be higher when the wind turbines are on. This is a bit tricky to evaluate because of the significant effect of wind speed. This dependence will be clarified in the next section.

⁴ A Health Canada scientist confirms that the turbines stopped turning completely when they were shut down during this cycling test. The operational logs, provided by the [REDACTED], also confirm this fact.

Third, there are harmonically-related spectral peaks evident when the wind turbines are on. For example, in Figure 22, the 15:45-16:45 interval has peaks at 0.6 Hz, 1.2 Hz, 1.8 Hz, 2.4 Hz, and 3 Hz. During this interval, the operational log reports a blade passage frequency of 0.6 Hz. These peaks are not evident during any of the "off" intervals. Therefore, the presence of such harmonically-related spectral peaks is associated solely with wind turbine noise emission.

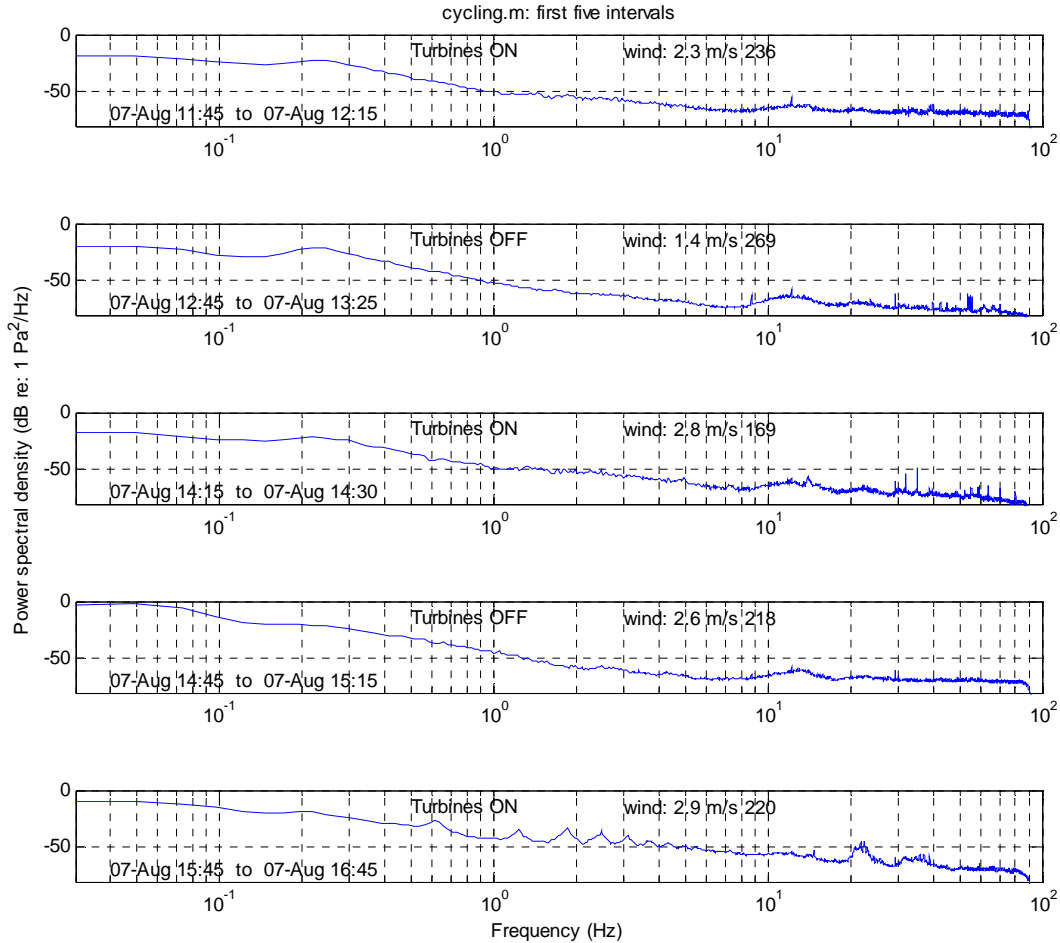


FIG. 22. Spectra for periods with wind turbines alternately on and off

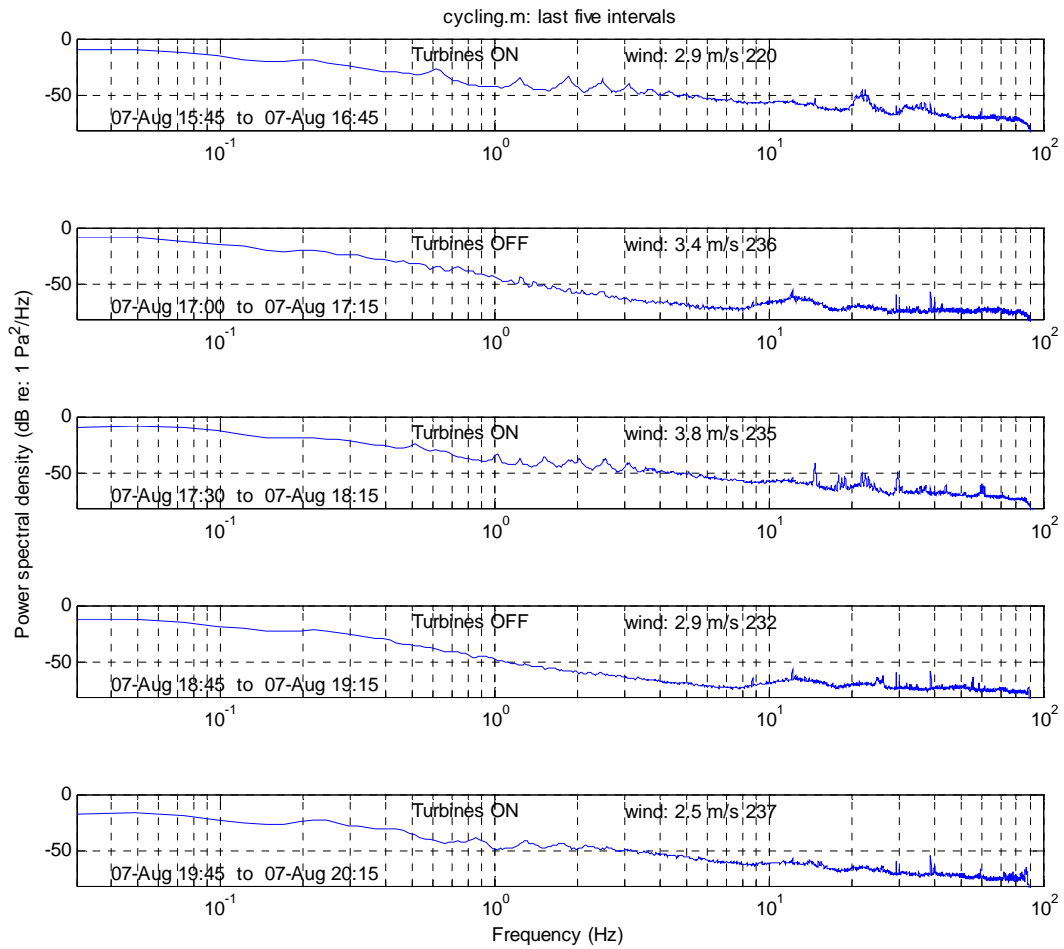


FIG. 23. Spectra for periods with wind turbines alternately on and off

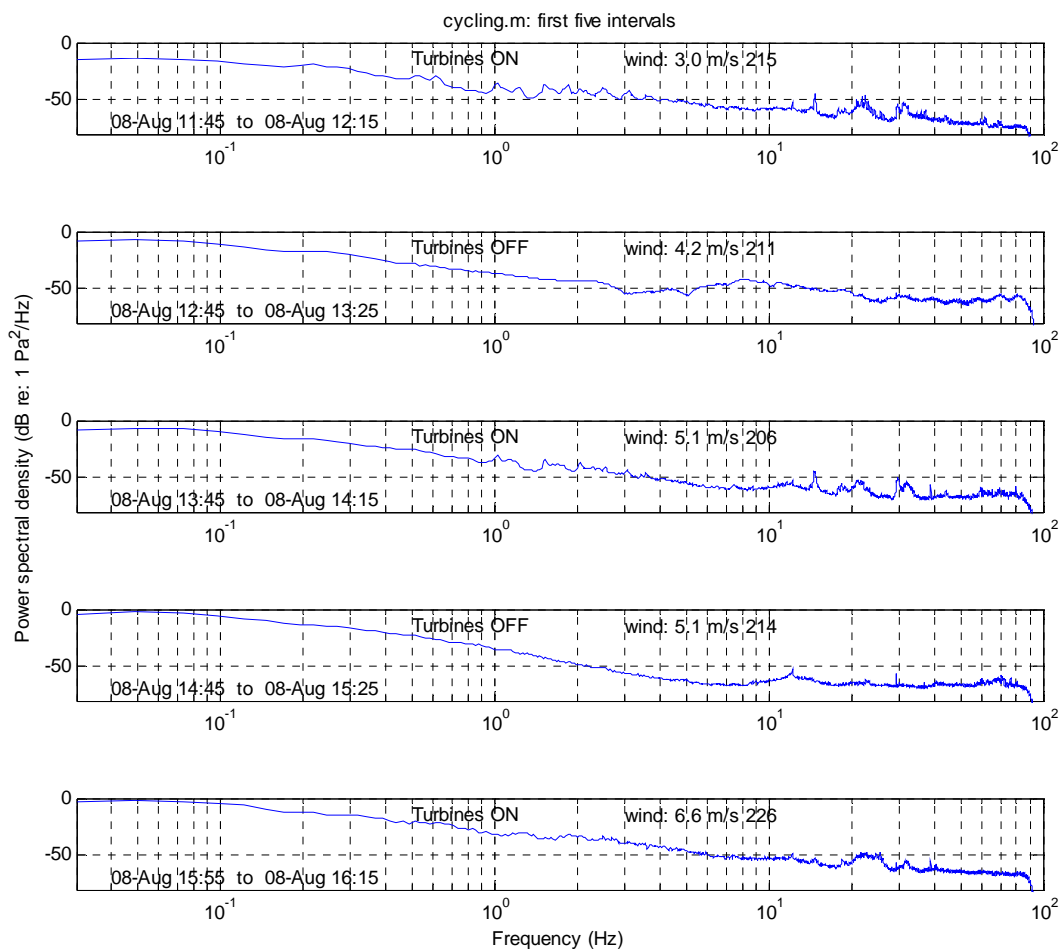


FIG. 24. Spectra for periods with wind turbines alternately on and off

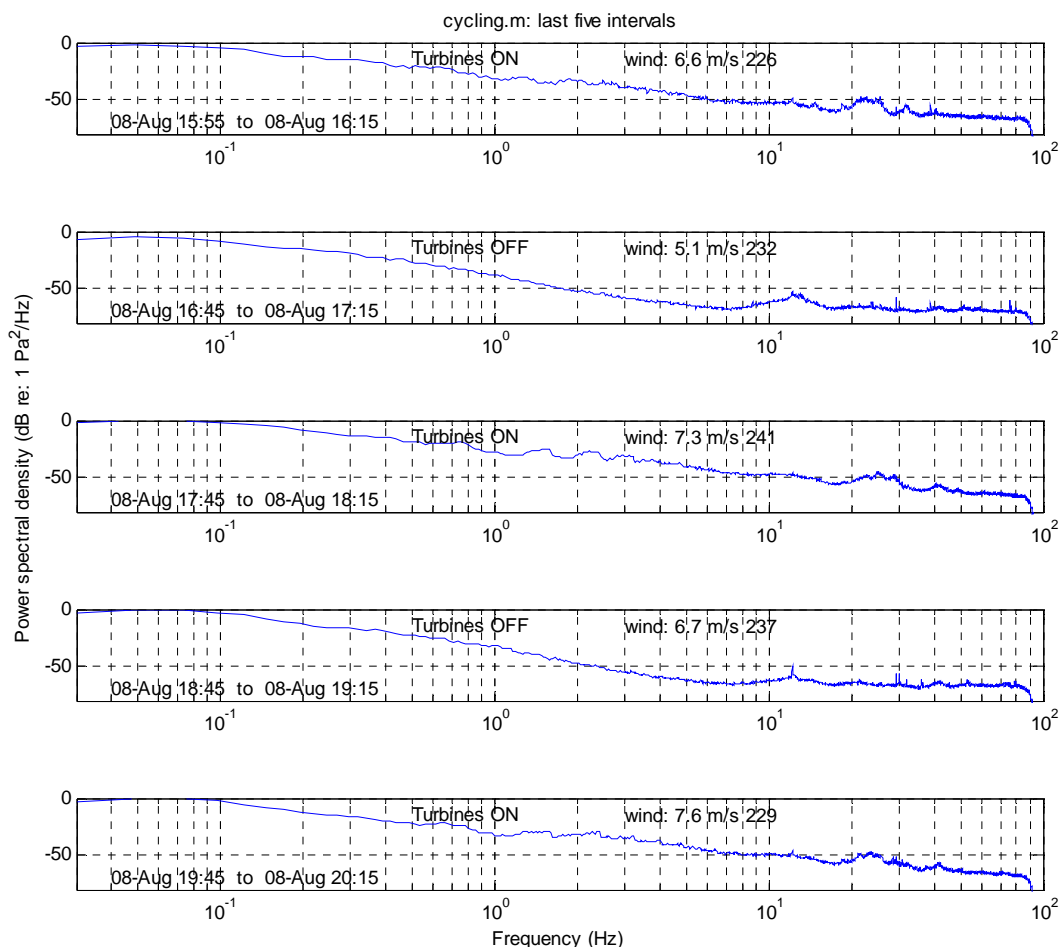


FIG. 25. Spectra for periods with wind turbines alternately on and off

To demonstrate the dependence of overall spectral level on wind speed, we plot in Figure 26 all the spectra obtained during an “off” interval. The thickness of the plotted line is varied in proportion to the wind speed, with lightest winds having the thinnest lines. A rough dependence is evident⁵.

⁵ A Health Canada scientist notes that a Hercules aircraft was performing “touch and go” manoeuvres over the turbines during one of the on/off cycles. We speculate that this could explain the 4.2 m/s curve which seems quite a bit higher than the other curves.

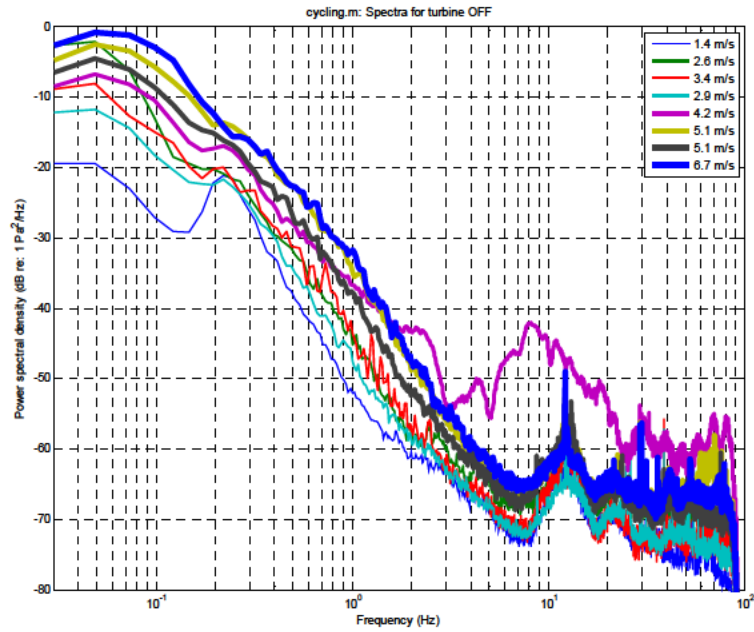


FIG. 26. Spectra for all periods with wind turbines off

Similarly, the spectra obtained during “on” intervals can be plotted together, in Figure 27. The spectra tend to be higher for the higher wind speeds.

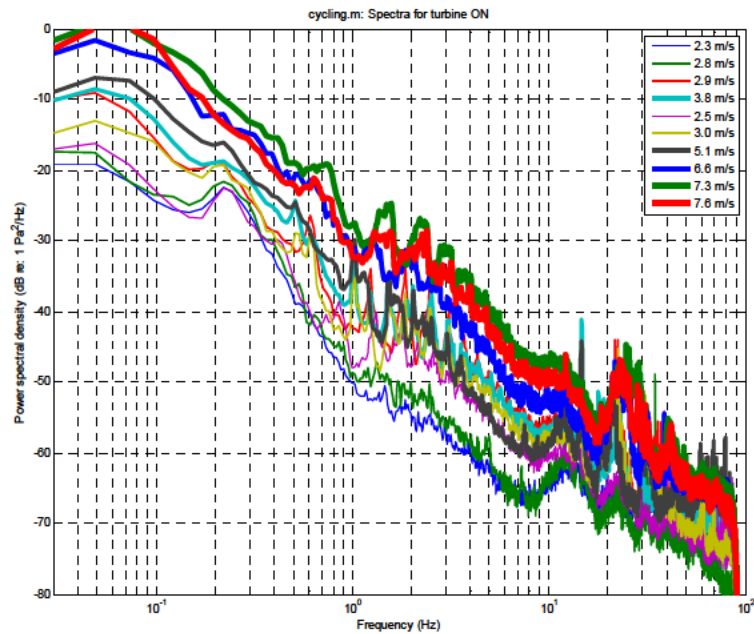


FIG. 27. Spectra for all periods with wind turbines on

It is noted that, except for the presence of the harmonically-related spectral peaks, the spectra for the wind turbine noise look very similar to the spectra for the ambient background noise.

During the night, the wind turbines were often idling because of the low wind speeds. Consider the interval between 2:00 and 3:00 on 8 August. For this stretch of one hour, the blade passage frequency of all wind turbines was 0.505 Hz, according to the operational logs provided by the [REDACTED]. The power spectrum corresponding to the sound pressure during this interval is shown below. Very sharp peaks are evident at frequencies that are multiples of the blade passage frequency. Clearly, the sharpness of the wind turbine peaks is related to the constancy of the blade passage frequency during the measurement period.

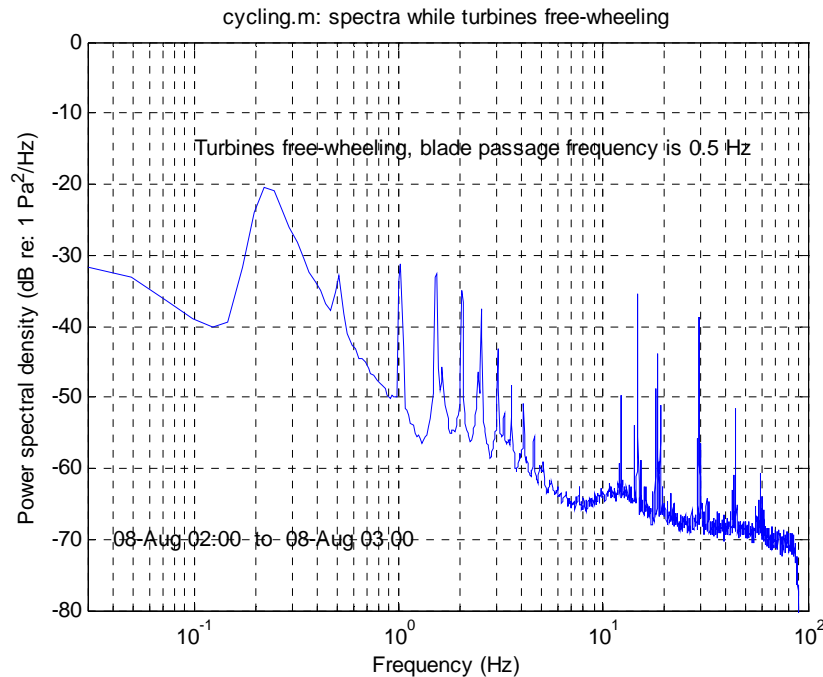


FIG. 28. Spectrum for wind turbines in idling mode

C. Separation of Wind Turbine Noise from Ambient Noise

By comparing successive intervals, we are able to extract the wind turbine noise component.

In Figure 29 below, we compare spectra obtained on 7 August for the interval 14:45 – 15:15 (off) and the following interval 15:45 – 16:45 (on). The wind speeds were similar, 2.6 m/s and 2.9 m/s⁶, and the wind directions were similar, 218° and 220°, so the dependence of spectra on the wind should be relatively unimportant. The individual spectra are shown in the top two panels. In

⁶ These wind speeds are below the nominal cut-in speed for the turbines so, ordinarily, the wind turbines would be idling at 10.1 rpm. However, as noted earlier, the [REDACTED] was operating the turbines under manual control and allowing them to turn with the wind at lower rpm.

the third panel, they are plotted together. There is nearly 15 dB separation between the two spectra between 1 Hz and 10 Hz. Therefore, in this frequency band, we can be sure that the "on" spectrum is mainly due to the wind turbines. Given this, we can subtract the "off" spectrum in an effort to get the turbine-only noise. The result is shown in the last panel.

As well as the harmonically-related peaks in the wind turbine spectrum, there are broad bands of noise centered about 22 Hz and 35 Hz. These are clearly associated with the wind turbines in some way, perhaps gear box noise.

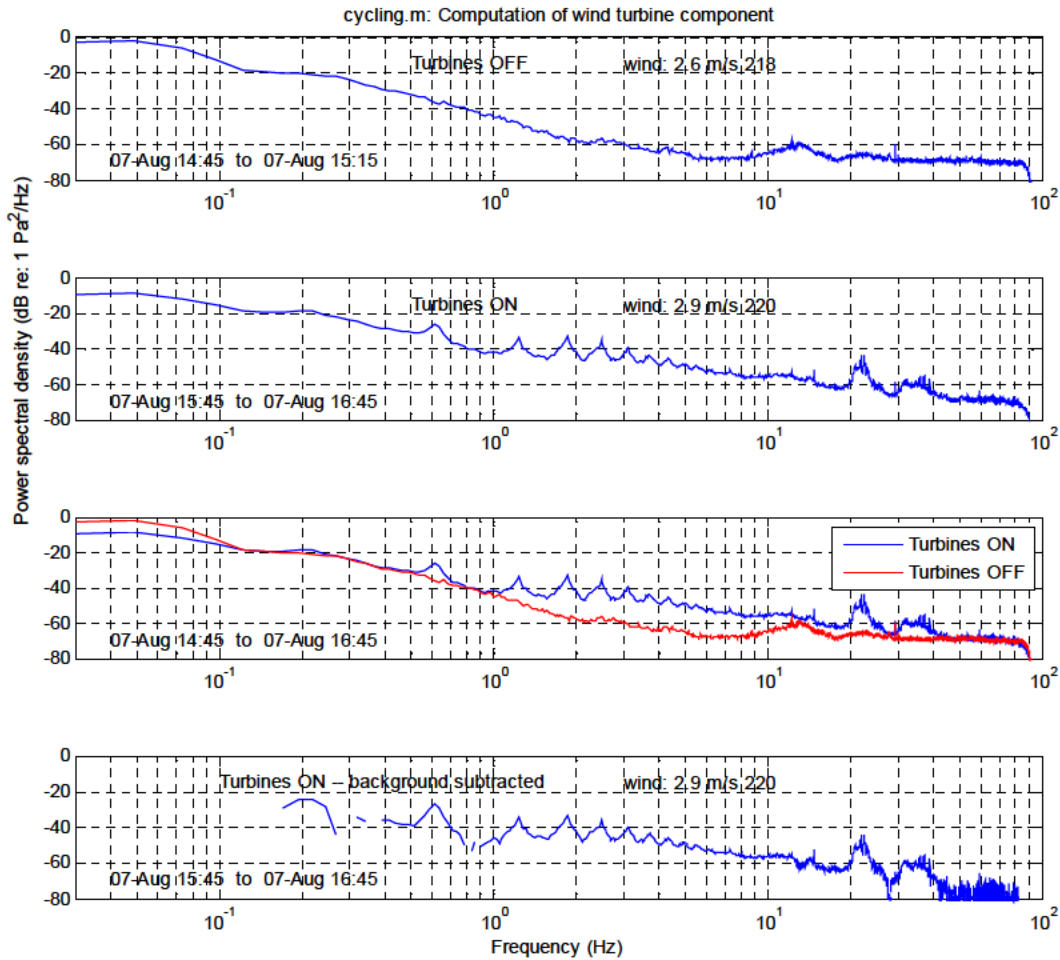


FIG. 29. Comparison of spectra for periods with wind turbines on and off

In the next example, we compare, in Figure 30, spectra for 8 August, intervals 18:45 - 19:15 (off) and 17:45 - 18:15 (on). The wind speeds are higher than for the previous example, being 6.7 m/s and 7.3 m/s; wind directions are 237° and 241°. For the "on" interval, the blade passage frequency is ranges between 0.7 Hz and 0.8 Hz. We see peaks at 1.5 Hz, 2.3 Hz and 3 Hz, in general agreement. These peaks are broader than in the previous example, presumably because of the changing blade passage frequency during the ½ hour interval.

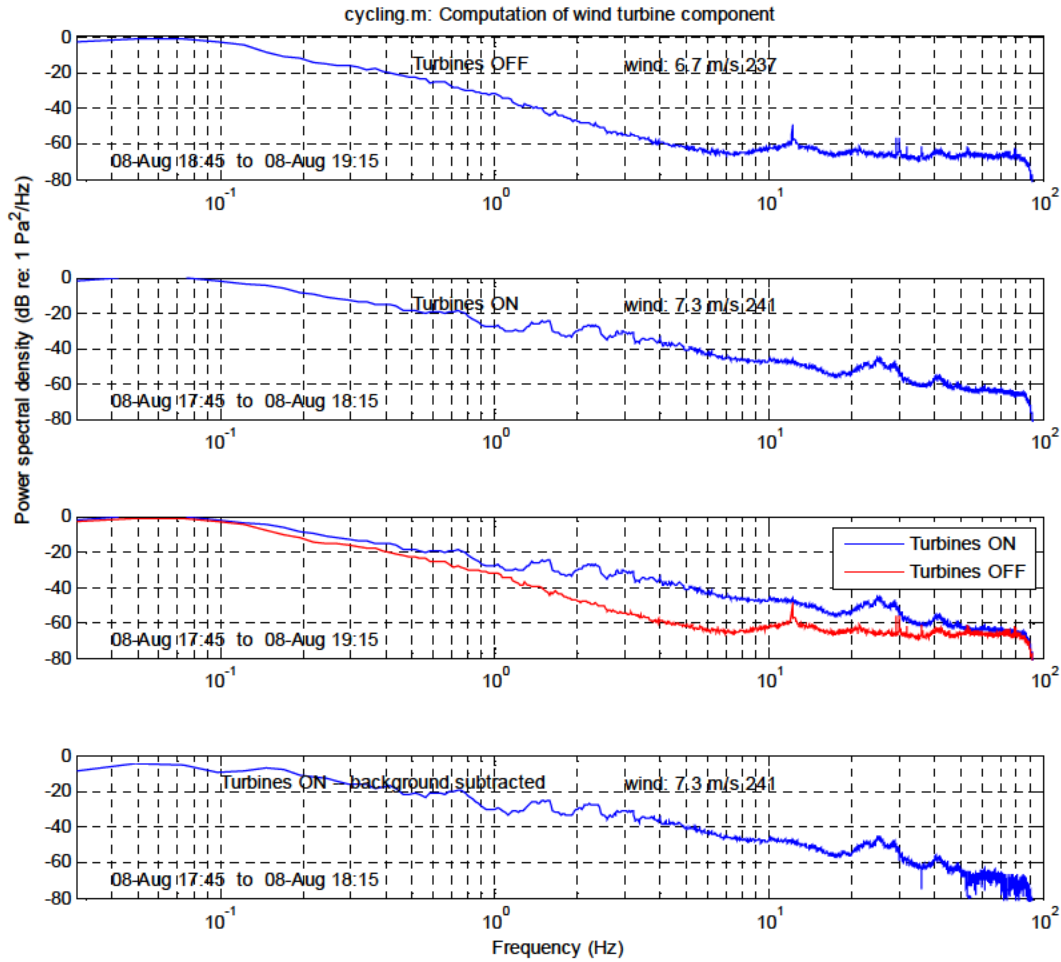


FIG. 30. Comparison of spectra for periods with wind turbines on and off

D. Directivity of Wind Turbine T2

To analyze the Health Canada measurements made on 7-8 August, a Matlab routine was written that allowed us to step forward and backward through the data one frame at a time. Each frame was 20 minutes.

An example of the graphical output is shown in Figure 31 below. The top left and top right plots show wind speed and direction, respectively, over the two day period. Red cross-hairs indicate the selected frame, i.e., time of data and corresponding values of wind speed and direction. The gray blocks on the abscissa of these two plots indicate periods for which the wind turbines were off. The top middle plot gives a top-view representation of the wind direction in relation to the three acoustical measurement positions (labeled "175 deg", "272 deg" and "310 deg"; these

positions located relative to true north) each 125 m away from the wind turbine T2. The bottom three plots show the computer power spectra for the selected time frame at each of the three measurement positions.

In this example, with the wind coming from 230°, there are harmonically-related peaks in the power spectra at all measurement positions. It is generally believed that noise emitted from wind turbines will show a dipole radiation pattern. Receivers upwind or downwind will be in a lobe (maximum) of the pattern while receivers crosswind will be in a null. For this wind direction, then, the “310 deg” position should be in a null and the peaks should be less. This might be the case here as the peaks do seem a couple dB lower than for the other two positions (and less background noise so peaks are more prominent).

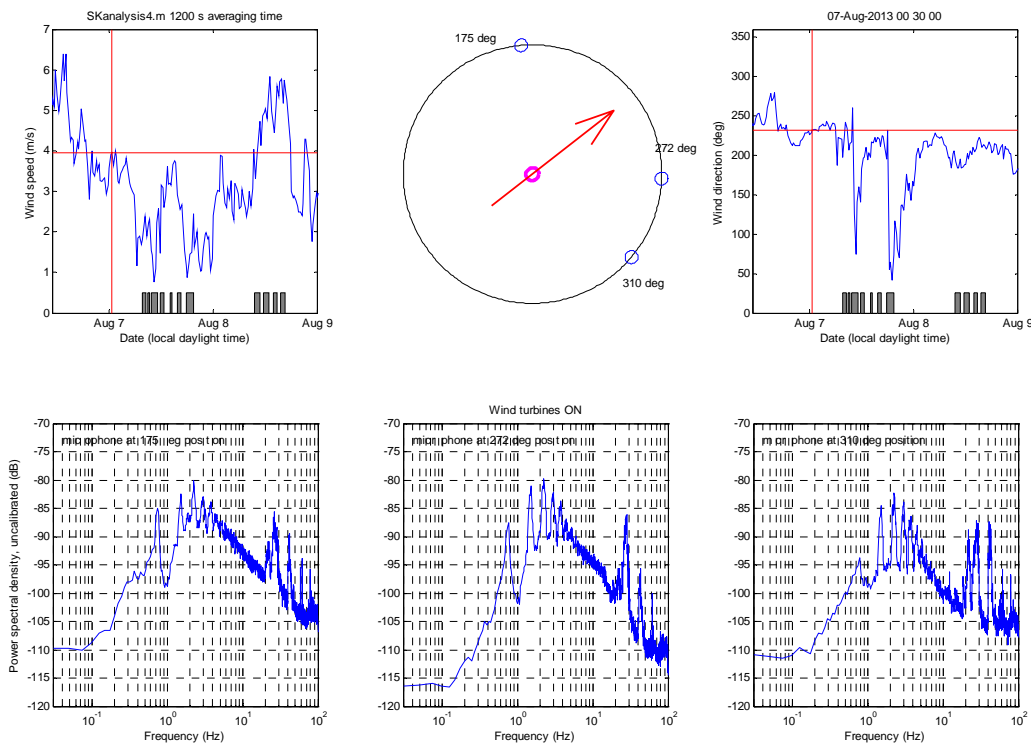


FIG. 31. Test of directivity

For the next example, in Figure 32, the wind is coming from 270°. The wind turbine noise would be expected to be loudest at the “272 deg” position, minimal at the “175 deg” position, and somewhere in between for the “310 deg” position. The spectra don’t support this assertion. The spectrum for “310 deg” is quite a bit higher overall than for the other two. Actually all three spectra are relatively high -- possibly there is another noise source that arose during this measurement frame.

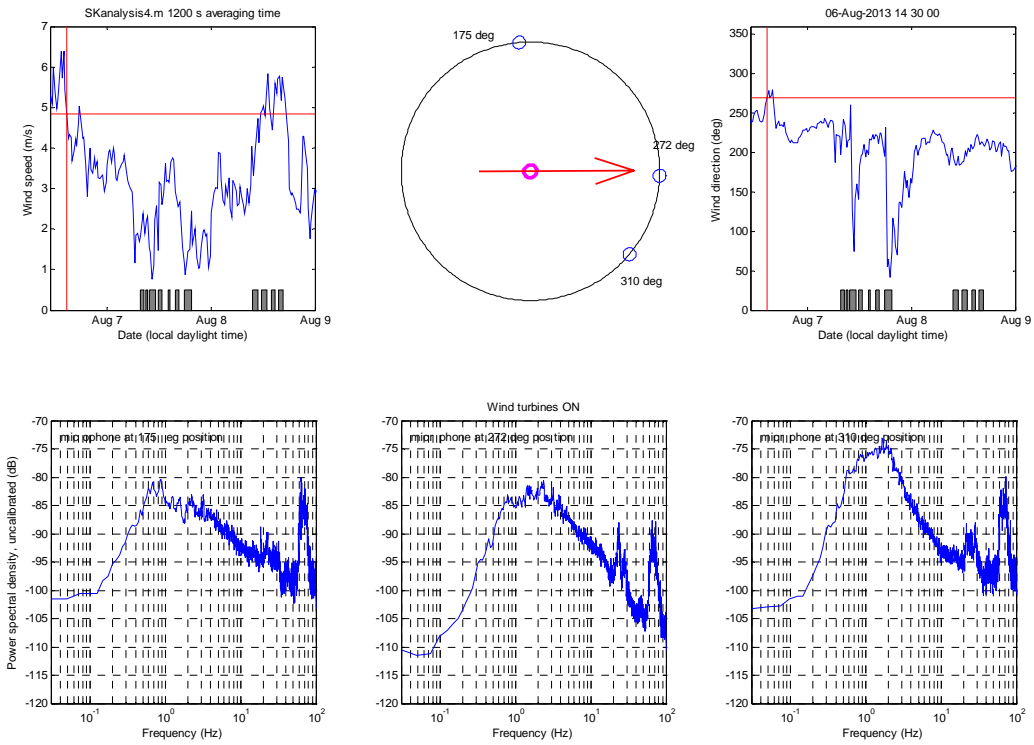


FIG. 32. Test of directivity

For wind coming from 310°, we have the following example in Figure 33,

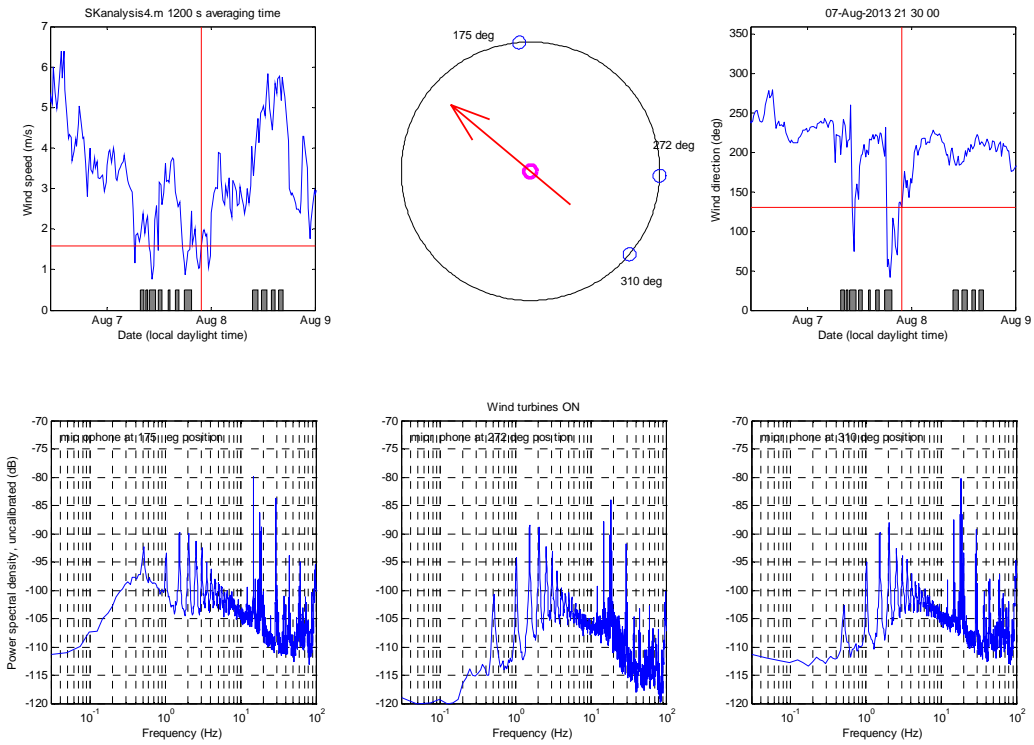


FIG. 33. Test of directivity

For wind from 195° , shown in Figure 34, would expect the peaks in the wind turbine spectra to be higher for the “175 deg” position and lower for the “272 deg” position. This could be so, although the spectra shapes are different, making assessment difficult.

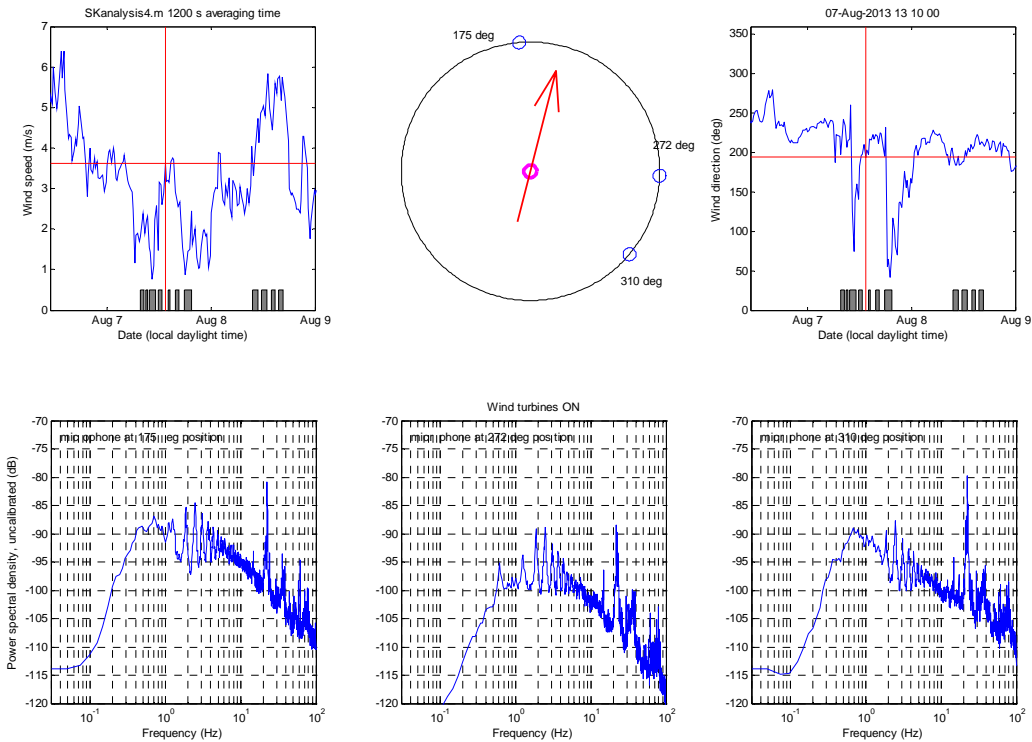


FIG. 34. Test of directivity

After reviewing hundreds of frames, tracking overall levels and specific spectral peaks, trying to fit data to functional forms involving wind direction and wind speed, we are not really able to make any strong conclusions. It does seem that any directionality of the wind turbines at low frequencies (say 1 Hz to 10 Hz) is not that strong, perhaps a few dB at most between lobe and null. There is also a sense that the maximum noise emission is not along the upwind/downwind direction but at some angle to this direction⁷.

⁷ A Health Canada scientist notes that some investigators have found the greatest emission of low frequency noise and infrasound at an angle of 45°.

VIII. PREPARATION FOR ACOUSTICAL CALCULATIONS

A. Computational Methods

For a study of the effects of infrasound from wind turbines, there is a need to predict the propagation of infrasonic frequencies up to large distances. However, engineering methods to predict the propagation of sound, such as those found in commercial software packages, were essentially developed for industrial noise, road and rail traffic noise. This puts into question the use of commercial software to predict the propagation of infrasonic frequencies.

For example, ISO 9613-2 is based on empirical corrections to inverse square law that are valid only down to 63 Hz. Further, ISO 9613-2 cannot accommodate a given sound speed profile.

More recent engineering methods such as the Nord2000 and the Harmonoise P2P models are more powerful. They can accommodate a number simplified sound speed profiles. However, for computational purposes, a linear fit is forced to the observed profile. This is because when the sound speed profile varies linearly with height, all the sound rays are given by the roots of a quartic equation and individual rays can be simply summed to obtain the overall sound pressure levels.

On the other hand, powerful computational models have also been developed that can accommodate any arbitrary sound speed profile. Examples of such computational models are the Parabolic Equation (PE) and the Fast Field Program (FFP). Both the PE and the FFP are based on numerical solution to the wave equation. Assuming simple harmonic time dependence $\exp(-i\omega t)$ the wave equation becomes the Helmholtz equation

$$(\nabla^2 + k^2)p(r, z) = -4\pi\delta(r, z - z_s)$$

where the wave number $k = \omega/c(z)$.

In the case of the PE, we begin with a change of variable $U = pr^{1/2}$ that leads to the Helmholtz equation for the field U in two dimensions (r, z) ,

$$\frac{\partial^2 U}{\partial r^2} + \frac{\partial^2 U}{\partial z^2} + k^2 U = 0$$

We define the operator Q as

$$Q = \frac{\partial^2}{\partial z^2} + k^2$$

Then the two dimensional Helmholtz equation can be written

$$\left(\frac{\partial}{\partial r} + i\sqrt{Q}\right)\left(\frac{\partial}{\partial r} - i\sqrt{Q}\right)U = 0$$

The factors represent propagation of incoming and outgoing waves respectively. Considering only the outgoing wave only, the above equation reduces to

$$\frac{\partial U}{\partial r} = i\sqrt{Q}U$$

The above equation is used for advancing the field in range and forms the basis for the PE methods.

Alternatively, the Helmholtz equation can be solved with a zero-order Hankel transform

$$p(r, z) = -\int_{-\infty}^{\infty} H_0^1(Kr)P(K, r)KdK$$

where H_0^1 is the Hankel function of the first kind of order 0. Writing the zero order Hankel transform as

$$p(r, z) = \int_0^{\infty} P(K, z)J_0(Kr)KdK$$

The above integral solution forms the basis for the FFP methods. In the FFP methods, the integral is solved numerically for the sound field $p(r, z)$ as a function of range.

B. Terrain data

Terrain elevation data files were downloaded from the GeoBase website, at www.geobase.ca.

For [REDACTED], PEI, and its environs, the relevant section is 011105. A corresponding zip file was downloaded and the two component subsections extracted:

011105_0100_demw.dem
011105_0100_deme.dem

These are east and west subsections of section 011105 and contain elevation data with a vertical resolution of 1 m. Each subsection gives a 1201×1201 array of elevation values with a horizontal resolution of 0.75 arcseconds. The ‘dem’ files are composed of header information in addition to the elevations, all in ASCII format. Matlab programs were written to read and decode the files.

The downloaded data corresponds to a region approximately $28 \text{ km} \times 35 \text{ km}$. This is more terrain than is necessary for the project at hand. A smaller region, approximately $7.5 \text{ km} \times 15 \text{ km}$, was extracted from the larger region.

The horizontal resolution of data points was approximately 23 m in the north-south direction and 16 m in the east-west direction. This is finer resolution than is needed for the sound propagation code, particularly given the relatively flat landscape around [REDACTED] and leads to unnecessarily large data arrays. A coarser resolution of 3 arcseconds was achieved by taking every 4th point, in both north-south and east-west directions. In the end, a 241×82 array of elevation values was obtained.

The terrain map obtained is shown in Figure 35.

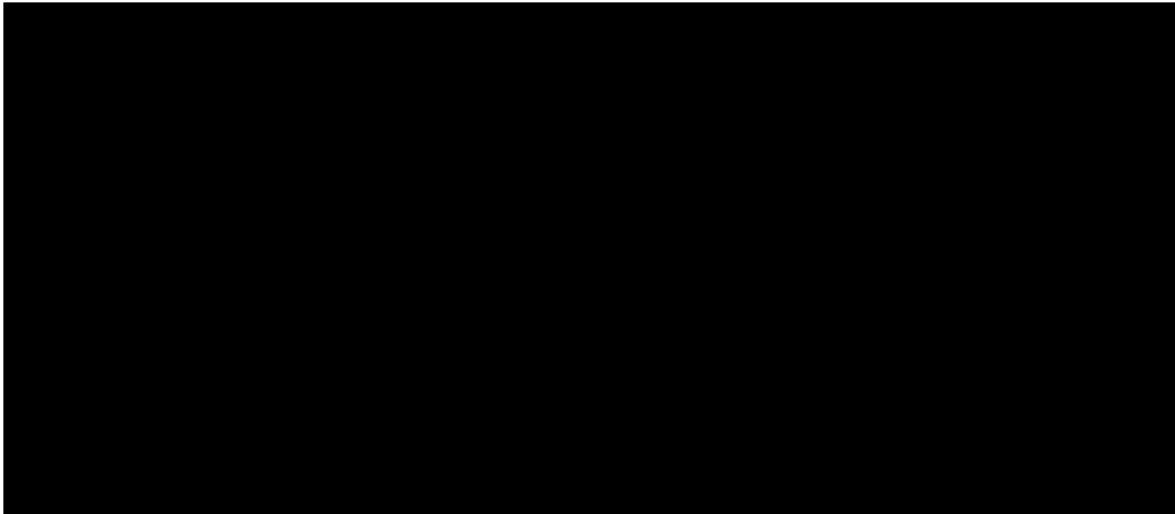


FIG. 35. Terrain map for sound propagation tests

In addition to the elevation data, shown by different colours in this plot, the location of the four wind turbines are indicated by the circled dots and the location of the measurement stations indicated with the blue circles.

The proprietary sound propagation code used by MG Acoustics requires that the elevation data be put into a Matlab ‘mat’ file with the appropriate structures and fields. A translation program was written to do this conversion.

Figure 36 below shows a sample sound map of the [REDACTED] site from one turbine.

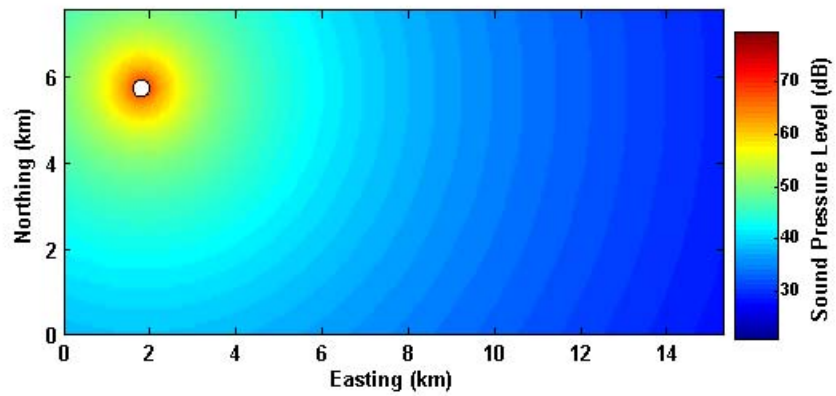


FIG. 36. Sound map for one wind turbine

The calculation was performed for a baseline condition (no refraction) at a frequency of 31.5 Hz using the data from Table 2.

IX. LONG RANGE PROPAGATION, THEORY VS. EXPERIMENT

In this Section, our numerical propagation codes will be applied to specific situations for which experimental results are reliable. Given the general difficulty separating wind turbine noise from ambient background noise, we will focus on the low frequency spectral peaks (below 8 Hz) that are clearly associated with the wind turbines, being harmonics of the blade passage frequency. The selection of data required that these spectral peaks be clearly evident (at least 5 dB above background) at all measurement stations (125 m, 2.5 km, 5 km, and 10 km ranges). This criterion was met relatively infrequently.

In the analysis of the measurement data, no initial assumption was made about the location in frequency of the spectral peaks. The data at the nearest measurement station (HC1P) were examined first. Spectra were computed from one hour time samples. The peaks were examined to find the harmonically-related frequencies at which the maxima occurred in the spectra. In all cases, these had a fundamental of 0.81 Hz. The spectral values at the same frequencies (e.g, 0.81 Hz, 1.62 Hz, ...) were then obtained for the other three measurement stations HC2P, HC3P, HC4P.

A. Analysis of 16 July 2013 data

On July 16th 2013, between 13:00 and 14:00 UTC, data shows clean signal at 2.4, 3.2, 4.0 and 4.8 Hz. Above 5 Hz, it is not possible to separate signal from noise.

The wind speed is 7 m/s at 10 m and is blowing towards the SW. The temperature difference $T(10\text{ m}) - T(2\text{ m}) \approx 0.5\text{ }^{\circ}\text{C}$ shows a weak inversion.

The temperature and wind speed profiles obtained from similarity and wind direction during the period are shown below in Figure 37.

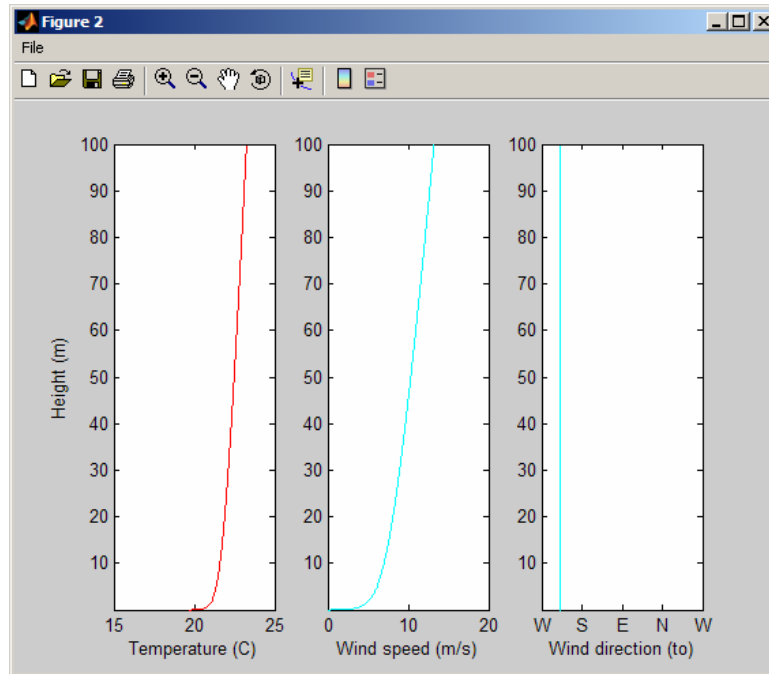


FIG. 37. Temperature, wind speed, and wind direction for selected time period

These profiles results in propagation that is partially upwind in the presence of a weak inversion. The effective sound speed profile is shown below in Figure 38.

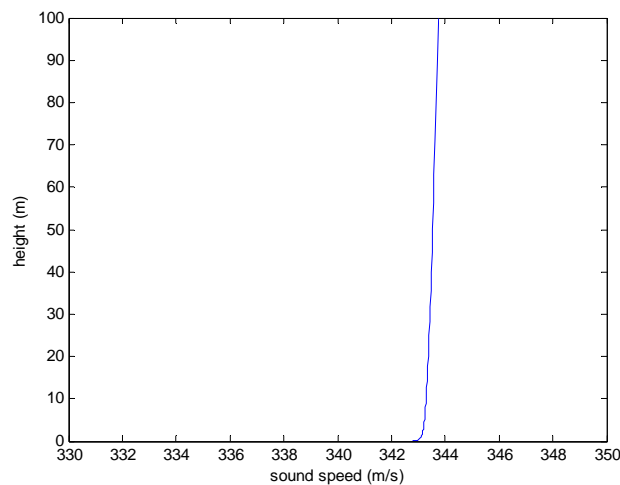
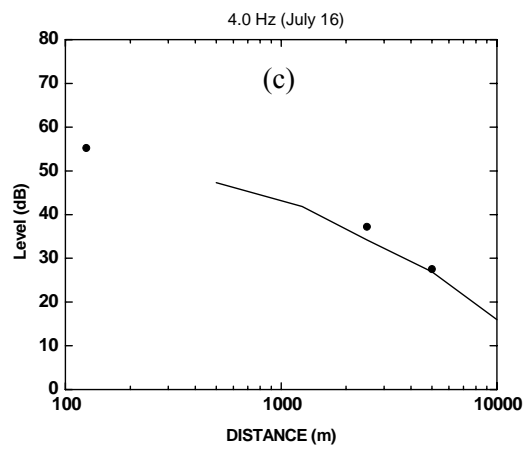
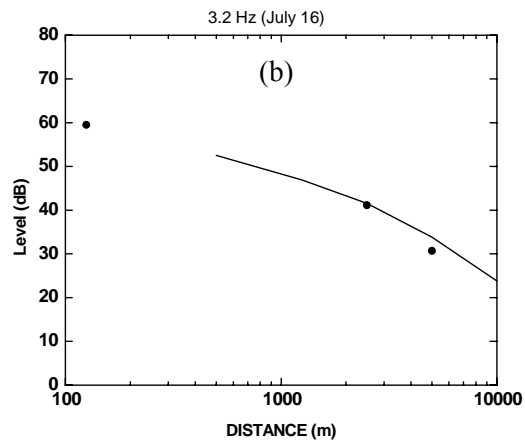
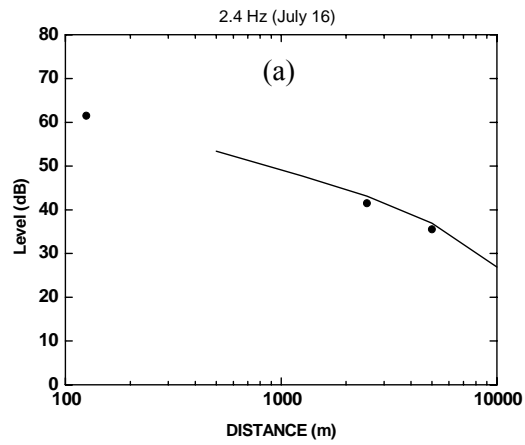


FIG. 38. Sound speed profile for selected time period

The profile shows a very weak variation with height, resulting in almost no refraction. This is fortunate. For this case, the Monin-Obukhov, $L > 100$ m and the similarity equations do not to yield reliable profiles above 100-200 m.

We found that the PE yielded predictions that agreed with data by using the atmospheric profiles up to a height of 100 m. The predictions at 2.4, 3.2, 4.0 and 4.8 Hz are shown below in Figure 39 (a)-(d).



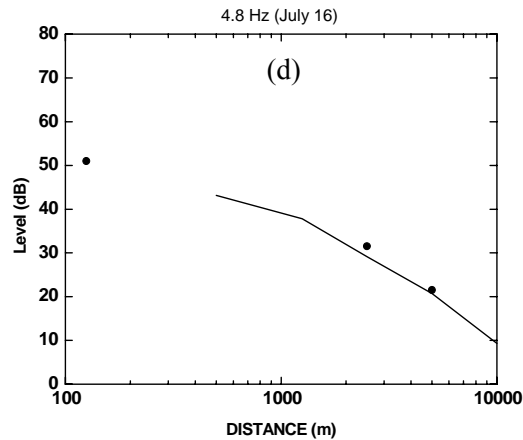


FIG. 39. Sound level variation with distance, prediction (line) versus measurements (circles)

For the above prediction, the signal measured at 125 m is used to determine the levels at turbine T2 using geometrical acoustics. Calculations confirmed that the levels measured at 125 m are from turbine T2 only, with the other three turbines very little to no contribution. Thus, the levels obtained at T2 are also used for the levels at the other three turbines.

The levels at each turbine are used in the PE to predict the levels as a function of distance, yielding the solid curves in the above four graphs. The calculations assume a ground impedance that is appropriate for a rural area with varied vegetation, but it should be noted that the ground impedance is a negligible factor at these low frequencies. A surface roughness of $z_o = 0.01$ m was used⁸. The levels measured at 125 m, 2.5 and 5 km are shown as the solid data points on the graphs. The agreement between predicted and measured levels is very good at all frequencies. Data was not available at 10 km.

B. Strong Inversion

The presence of a strong inversion was encountered during a series of nights between June 2013 and September 2013. The data recorded at the meteorological tower and averaged over 1 hour are listed below.

11 June 2013 (05:00 to 06:00)

$$T(10 \text{ m}) - T(2 \text{ m}) = 1.4 \text{ }^{\circ}\text{C}$$

$$\text{Wind (10 m)} = 5.0 \text{ m/s from } 240^{\circ}$$

11 June 2013 (06:00 to 07:00)

$$T(10 \text{ m}) - T(2 \text{ m}) = 1.3 \text{ }^{\circ}\text{C}$$

$$\text{Wind (10 m)} = 4.6 \text{ m/s from } 237^{\circ}$$

⁸ This is a commonly used default value. It is a non-critical parameter for our purposes here.

23 June 2013 (04:00 to 05:00)
T(10 m) – T(2 m) = 0.9 °C
Wind (10 m) = 5.6 m/s from 234°

23 June 2013 (05:00 to 06:00)
T(10 m) – T(2 m) = 0.9 °C
Wind (10 m) = 5.6 m/s from 234°

23 June 2013 (06:00 to 07:00)
T(10 m) – T(2 m) = 0.9 °C
Wind (10 m) = 5.8 m/s from 237°

1 August 2013 (02:00 to 03:00)
T(10 m) – T(2 m) = 2.0 °C
Wind (10 m) = 5.2 m/s from 233°

1 August 2013 (03:00 to 04:00)
T(10 m) – T(2 m) = 1.7 °C
Wind (10 m) = 5.4 m/s from 235°

1 August 2013 (04:00 to 05:00)
T(10 m) – T(2 m) = 1.6 °C
Wind (10 m) = 4.9 m/s from 237°

19 August 2013 (04:00 to 05:00)
T(10 m) – T(2 m) = 1.6 °C
Wind (10 m) = 6.8 m/s from 243°

28 September 2013 (23:00 to 00:00)
T(10 m) – T(2 m) = 1.4 °C
Wind (10 m) = 4.7 m/s from 231°

The temperature differences, wind speeds and directions are comparable on all 10 nights.

The propagation to the sensors is downwind, and with the presence of the inversion, strong downward refraction yields strong signals at a number of frequencies. An example of the acoustic data for the period 05:00 to 06:00 on June 11th is shown below in Figure 40. The spectral peaks are well above the background levels -- they are believed to be very reliable. Data was extracted for 1.61, 2.42, 3.22, 4.03, 4.83, and 5.64 Hz. At higher frequencies, ~20, ~45, and ~70 Hz, there are consistent broad peaks in the spectra at all four ranges that are assumed to be associated with the wind turbines. These are analyzed as well.

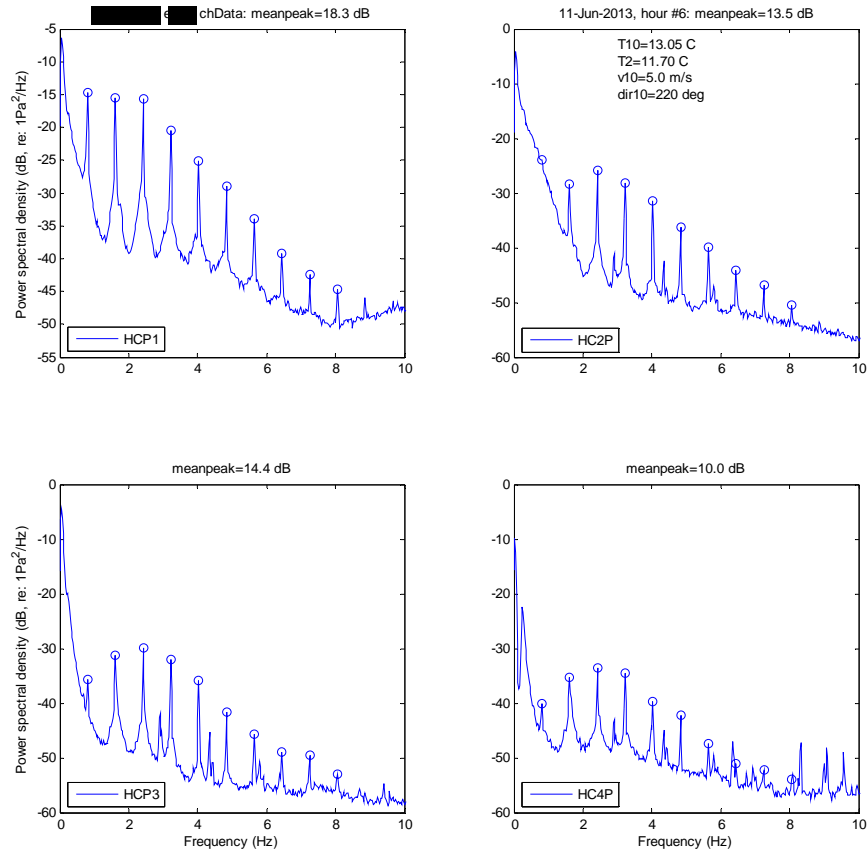


FIG. 40. Spectra at the four measurement stations, showing distinct peaks arising from the wind turbines

Unfortunately, similarity does not provide reliable profile above 100-200 m for these strong inversion conditions. Shown below in Figure 41 are the temperature and wind speed profile up to a height of 1 km. They are unrealistic above 200 m.

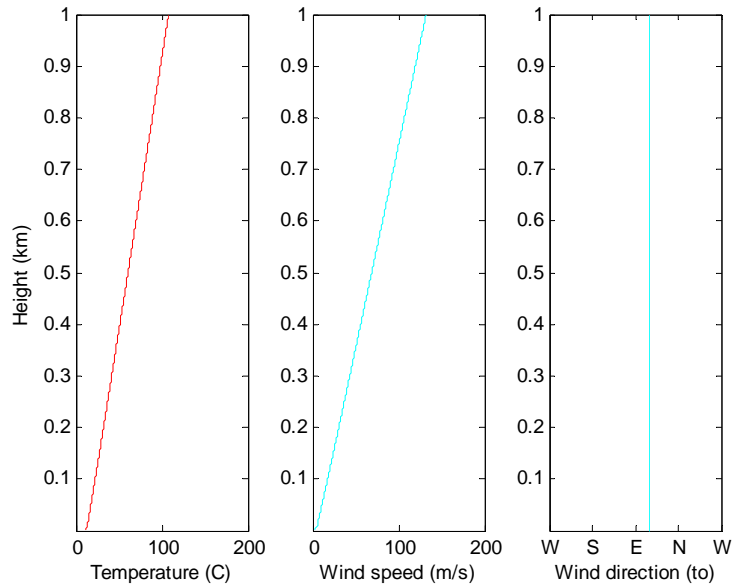


FIG. 41. Temperature, wind speed, and wind direction for selected time period

The resulting effective sound speed profile is shown in Figure 42. The profile above about 200 m is also totally unrealistic.

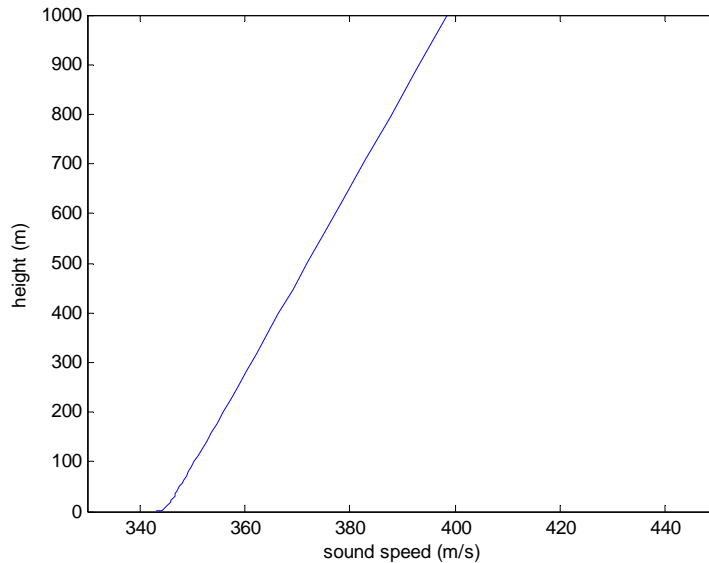


FIG. 42. Sound speed profile for selected time period

If the above sound speed profile is used to launch rays, the ray picture shown below in Figure 43 is obtained. We note that a majority of rays are found below about 100 m at the shorter distances and below about 200 m by 10 km. This implies the profiles obtained from similarity below about 200 m could yield reliable predicted levels.

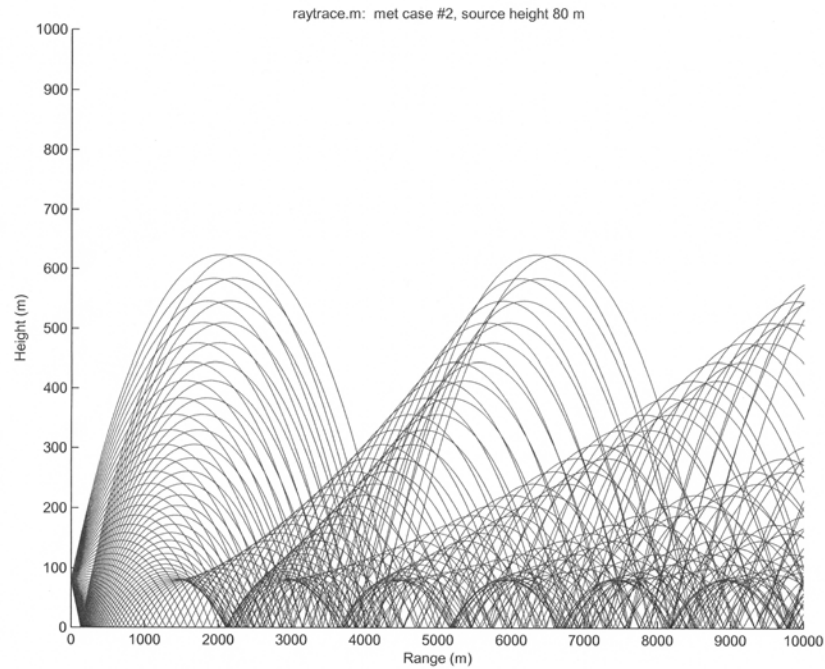


FIG. 43. Ray trajectories for the sound speed profile of the previous figure

Because the profile varies strongly with height for these inversion cases, fine tuning of the Fast PE is required resulting in excessive computing time. Therefore, the Fast Field Program (FFP) was used to calculate sound levels for these cases. We found that sound levels began to converge when the sound speed profile was capped at about 200-250 m, confirming that most of the energy arrives from rays below about 200 m. An example of transmission loss for turbine T2 is mapped in Figure 44 below (frequency of 4.03 Hz). Levels as a function of distance are computed using the transmission loss and the levels measured at 125 m, as explained earlier.

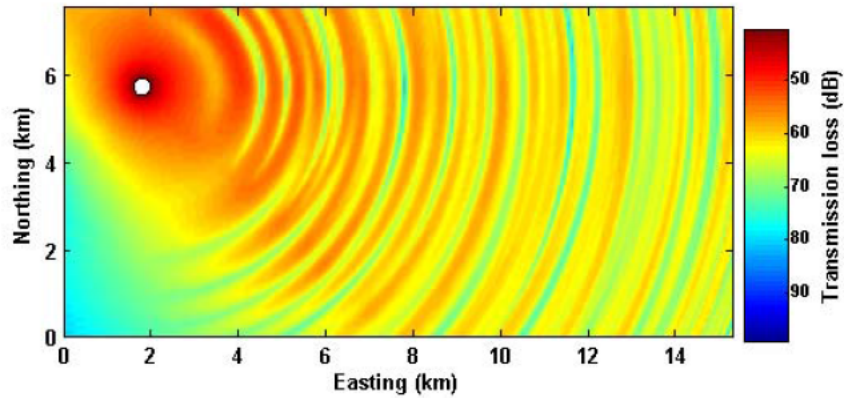
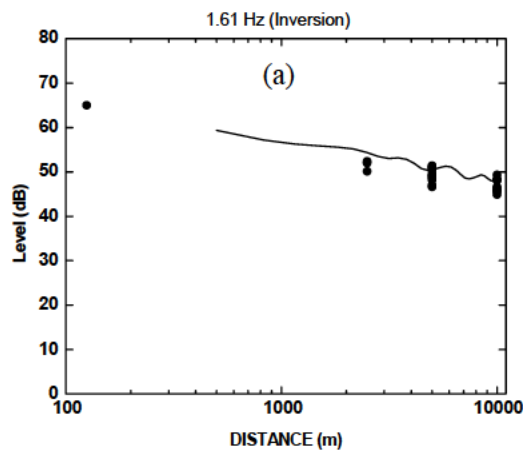
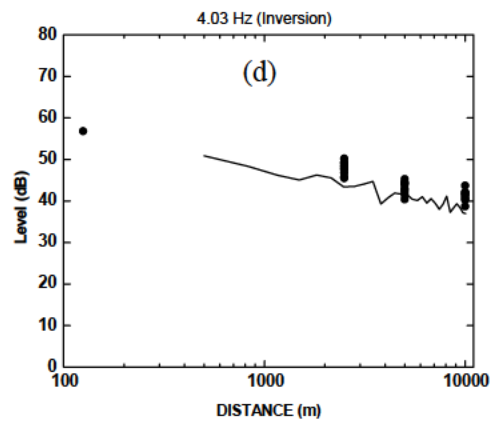
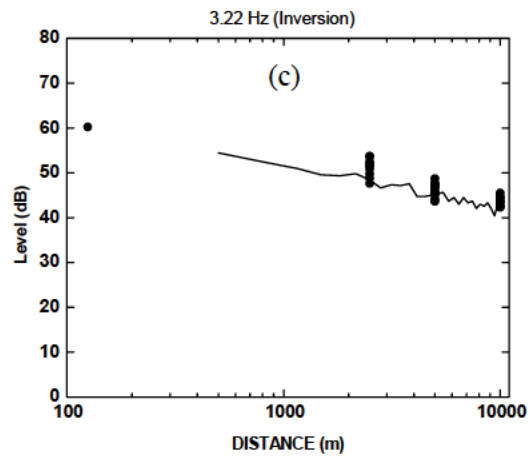
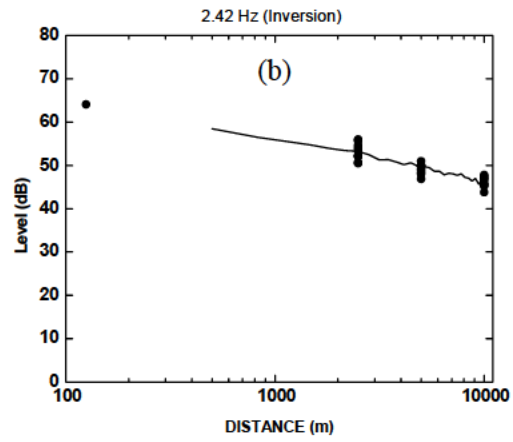


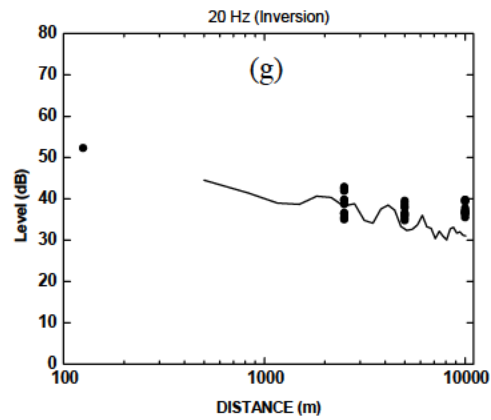
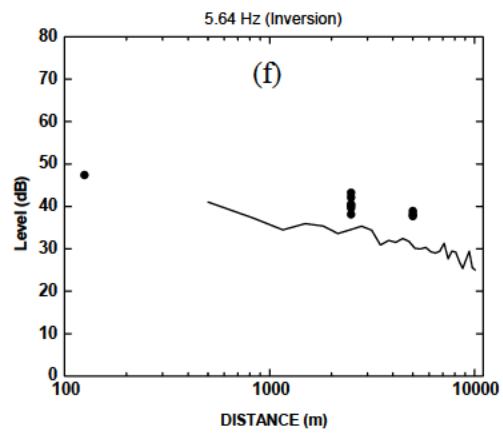
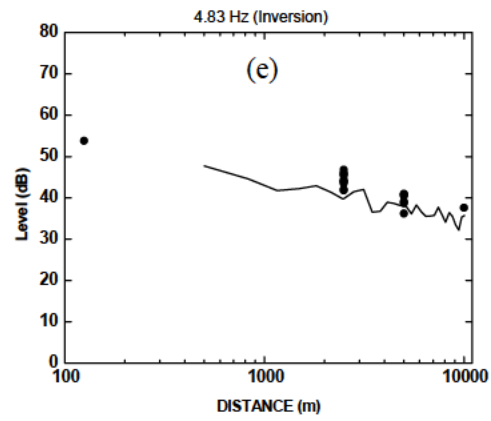
FIG. 44. Sound map for wind turbine T2, downward refracting conditions

For the computation, the meteorological data from June 11th (05:00 to 06:00) was used in similarity as representative of the average conditions during the 10 nights. The levels at 125 m (from T2) were averaged over the 10 nights at each frequency and the average value used to determine the nominal levels at each turbine. These nominal levels were used with the FFP results to compute the predicted levels at each frequency.

The curves in the Figure 45 (a)-(i) are the predicted levels as a function of distance for the nine frequencies of 1.61, 2.42, 3.22, 4.03, 4.83, 5.64, ~20, ~45, and ~70 Hz. The solid points are the individual measured levels available from the 10 nights for the 9 frequencies for the various periods.







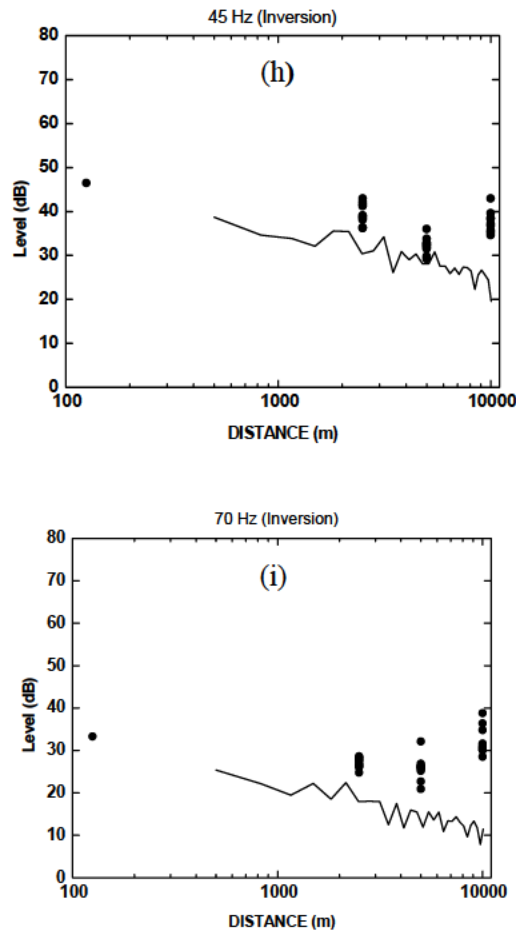


FIG. 45. Sound level variation with distance, prediction (lines) versus measurements (circles)

The agreement between predicted and measured levels is good at 1.61, 2.42, and 3.22 Hz at 2.5, 5 and 10 km. At 4.03 and 4.83 Hz, we note the measured levels at 2.5 km are generally higher than the predicted levels. At 5.64 Hz, the measured levels at 2.5 and 5 km are generally higher than the predicted levels.

At 20 Hz the agreement between measured and predicted levels is good at 2.5 and 5 km. At 10 km, the measured levels are generally higher than the predicted levels. At 45 Hz, the measured levels at 2.5 km are generally higher than the predicted levels while the agreement between measured and predicted levels seems reasonable at 5 km. The measured levels at 10 km suggest the presence of significant background noise contributing to the signal. Note that the flow resistivity of the ground was increased, giving a ground impedance appropriate to “soil”, to provide slightly better fit to the measured levels at 20 and 45 Hz.

At 70 Hz, the measured levels are notably higher than the predicted levels at all three further distances, suggesting that background noise is contributing significantly to the signal.

C. Analysis of 18 June 2013 data

On June 18th (18:00 to 19:00 UTC), the wind was blowing almost due East with a speed of 8.4 m/s and there was a temperature lapse with $T(10\text{ m}) - T(2\text{ m}) = -0.5\text{ }^{\circ}\text{C}$. The wind speed and temperature profiles are shown in Figure 46. Note that in this case similarity produces profiles that are well behaved up to a height of 1 km.

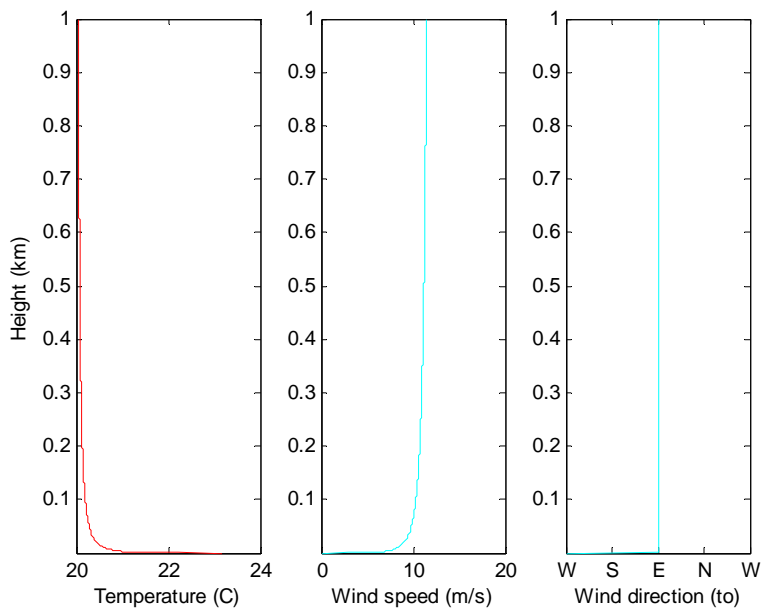


FIG. 46. Temperature, wind speed, and wind direction for 18 June 2013

The resulting effective sound speed profile is shown below in Figure 47.

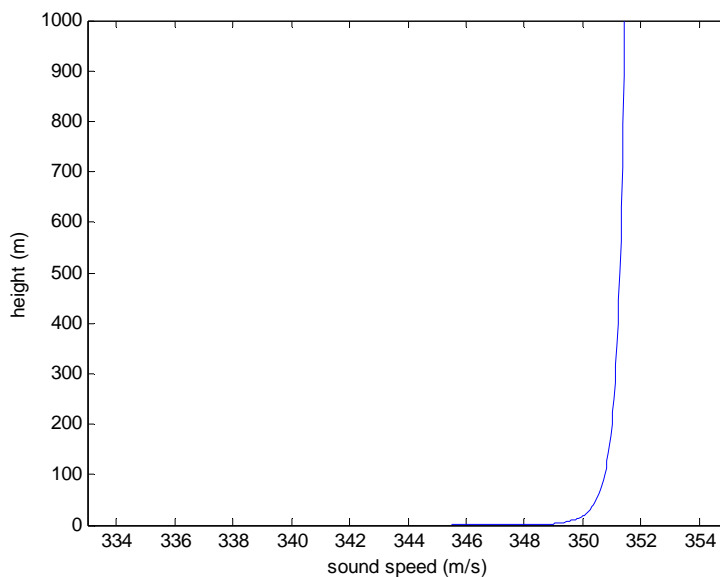


FIG. 47. Sound speed profile, 18 June 2013

The predicted levels at 3.2 Hz, 5.6 Hz, and 20 Hz are shown by the curves in Figure 48 (a)-(c).

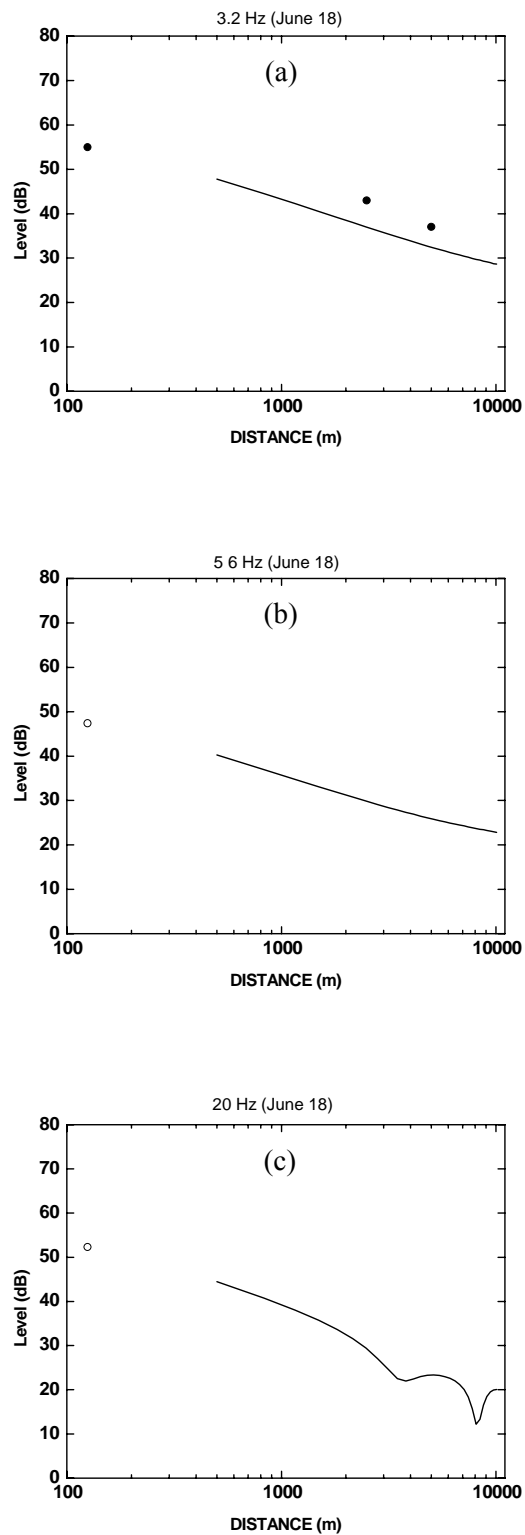


FIG. 48. Sound level variation with distance, prediction (lines) versus measurements (circles)

Measured data was available at 3.2 Hz and is shown by the solid points. The agreement between measured and predicted levels is marginal, with the measured levels being about 4-5 dB higher than the predicted levels. No data was available at 5.6 and 20 Hz. For the calculations, the levels at turbine T2 at 125 m from June 11 showed by the open points were used for the predictions.

D. Examples of predicted levels obtained from similarity versus stability classes

In Section IV, a number of profiles obtained from similarity and stability classes were compared. Considerable differences were found in some cases. For example we reproduce in Figure 49 the profiles obtained on the 14th of July, but here only plotted up to 200 m.

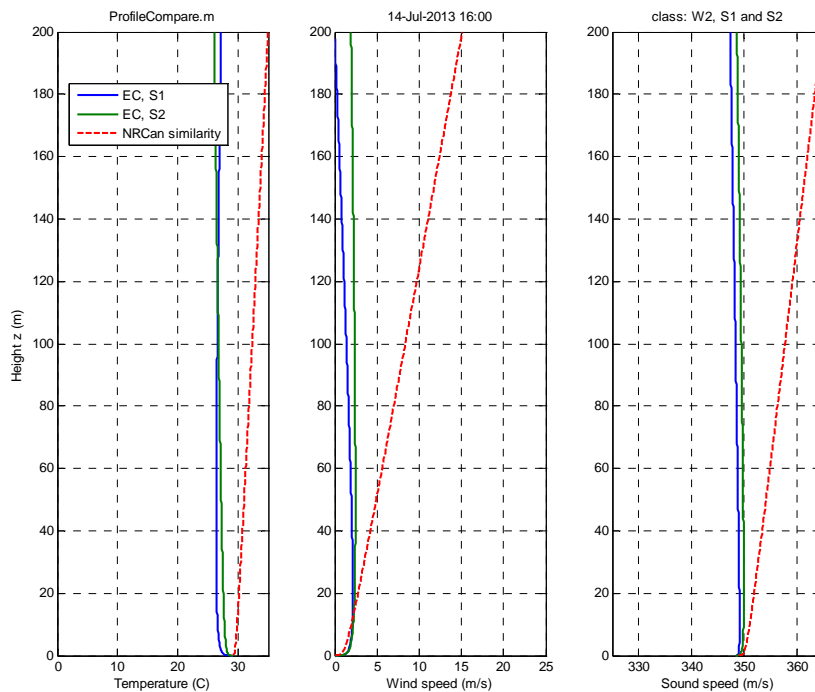


FIG. 49. Temperature, wind speed, and sound speed profiles, for 14 July 2013

The raw data for this day and time is as follows

14 July, 16:00

From Environment Canada,

$T(10m)=31.4$ deg

$v(10m)=1.94$ m/s

$dir(10m)=280$ deg

As discussed previous, this corresponds to a wind class of W2 and a stability class S1 or S2

From met tower at HC2P

$T(10\text{m})=29.8$ deg

$T(2\text{m})=29.5$ deg

$v(10\text{m})=1.96$ m/s

$\text{dir}(10\text{m})=321$ deg

The following Figure 50 compares the levels predicted using the profiles obtained from similarity versus the levels predicted using profiles obtained from stability classes (calculated for stability class S2; using class S1 would give almost the same result) for a frequency of 4.8 Hz. The differences become important beyond about 1 km.

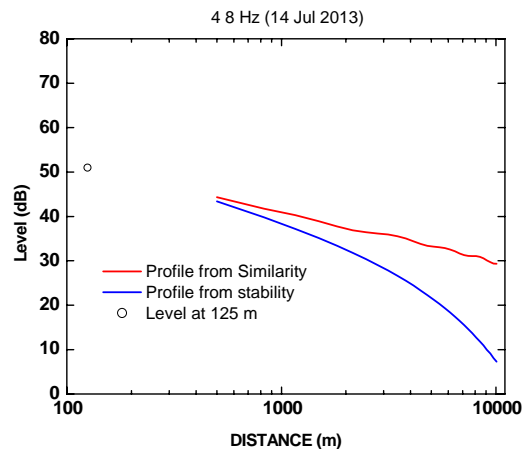


FIG. 50. Predicted sound level variation, for sound speed profiles calculated using similarity and using a weather class (stability) approach

Note that a similar situation occurs on the 9th of October (see Section VI) with the exception that the form of the profiles between similarity and stability classes are reversed. Thus, in the case of predicted levels on the 9th of October, stability classes would yield the red curve in Figure 50, while similarity would yield the blue curve.

Similarity is an approximation based on long-term averages of a complicated dynamic system. The stability-based approach used by Nord2000/Harmonoise makes further approximations and simplifications. So, similarity may be the better approach. The stability -based approach has been considered here because it could be a backup approach for situations in which the meteorological equipment necessary to apply similarity is not available. Neither approach is expected to yield valid sound speed profiles at heights above 100 or 200 m; with the 10-1 rule of thumb, calculated sound propagation beyond 1 km range becomes more uncertain. Clearly, the only way to resolve the expected levels beyond 1 km in these two cases would be to use meteorological data obtained from weather balloons, SODAR, etc.

E. Analysis of November 2013 data

On November 15th (21:00 to 22:00 UTC), the wind was blowing towards the NNE with a speed of 5.0 m/s. The temperatures at 2 m and 10 m were 6.1°C and 7.8°C, respectively. The resulting sound speed profile is shown in Figure 51 below.

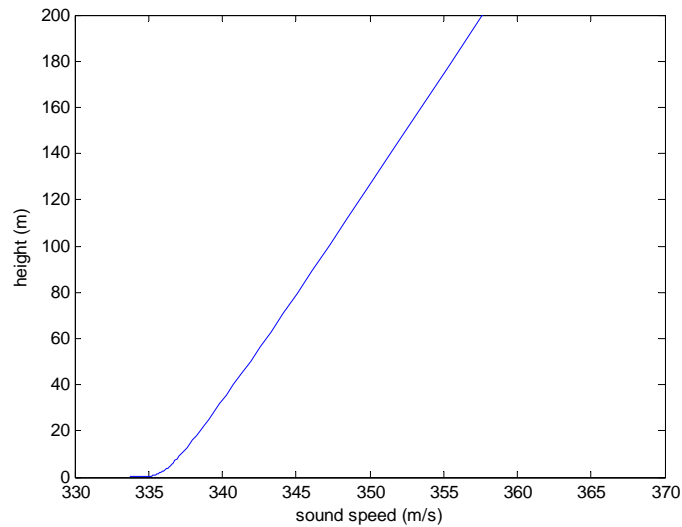
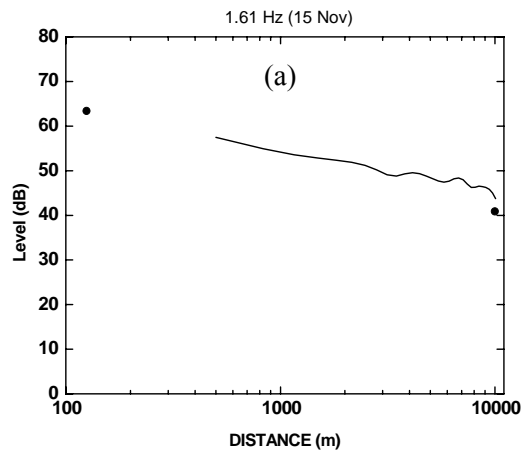


FIG. 51. Sound speed profile, 15 November 2013

This again corresponds to an inversion condition, but the inversion is deeper than those measured during the late Fall (June) and Summer (August and September) months discussed earlier.

The predicted levels at 1.61 Hz, 2.42 Hz, 3.22 Hz, and 4.03 Hz are shown below in Figure 52 (a)-(d). Note the measured results have been corrected for background noise since in most cases the SNR was less than 10 dB.



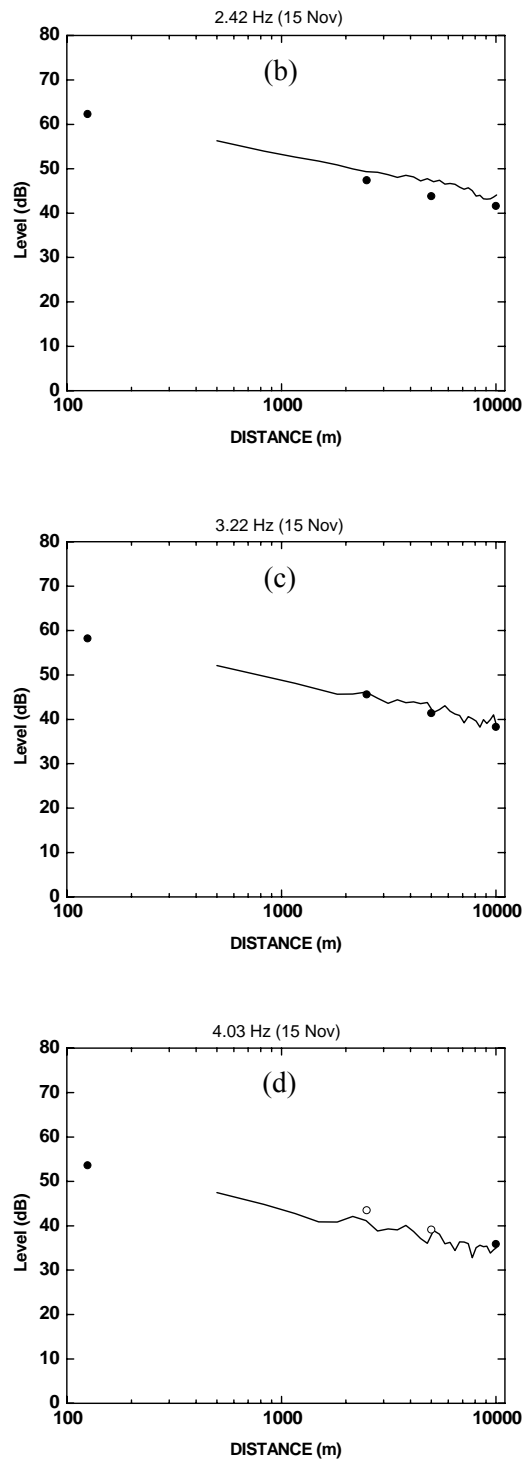


FIG. 52. Sound level variation with distance, prediction (lines) versus measurements (circles), 15 November 2013

Although the inversion is deeper, the measured and predicted levels compare well to results shown earlier during inversion conditions between the months of June and September. The open

circles for 4.03 Hz at 2500 m and 5000 m indicate that the results did not meet the selection criteria. However, the SNR is very close to 10 dB and they are included for completeness, but they have not been corrected for background noise.

On November 21st (23:00 to midnight), the wind was blowing towards the ESE with a speed of 4.6 m/s. The temperatures at 2 m and 10 m were 0.9°C and 2.6°C, respectively. The resulting wind speed profile is shown in Figure 53.

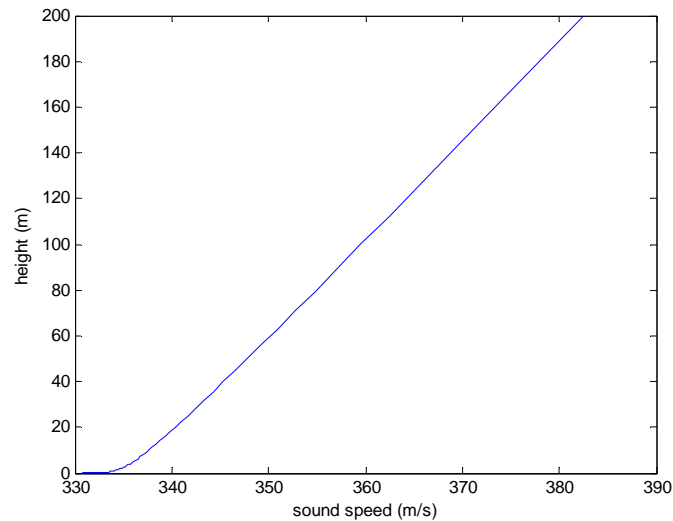
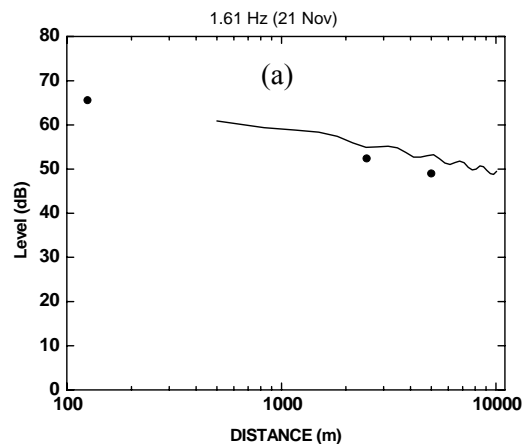
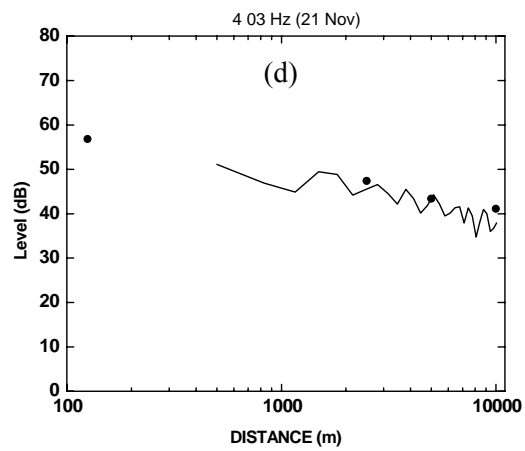
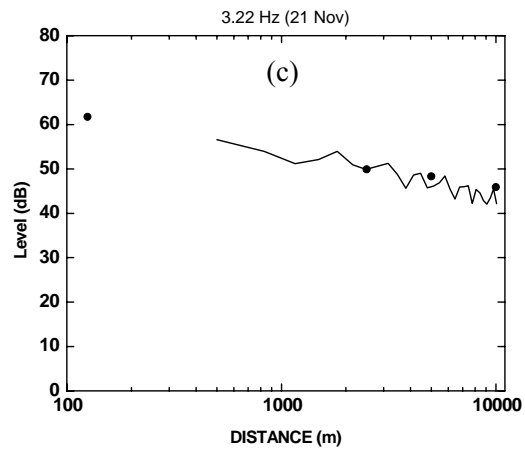
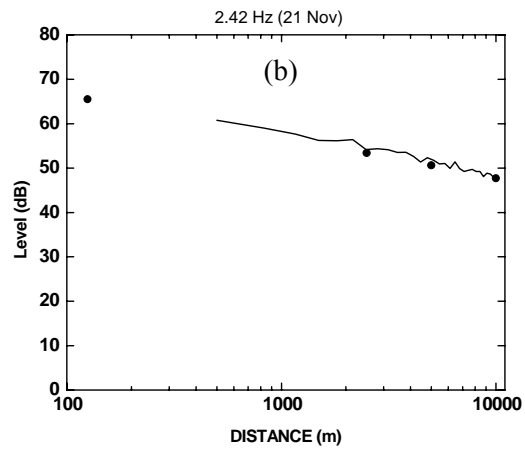


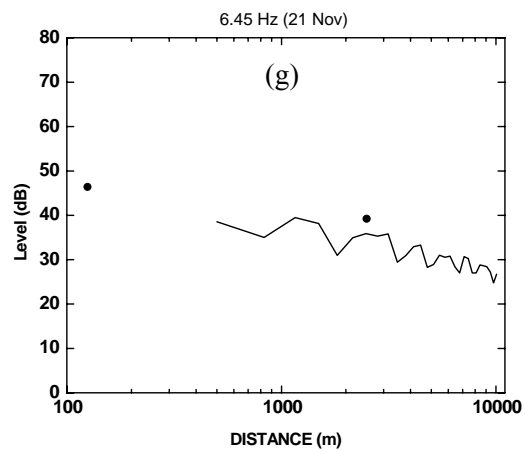
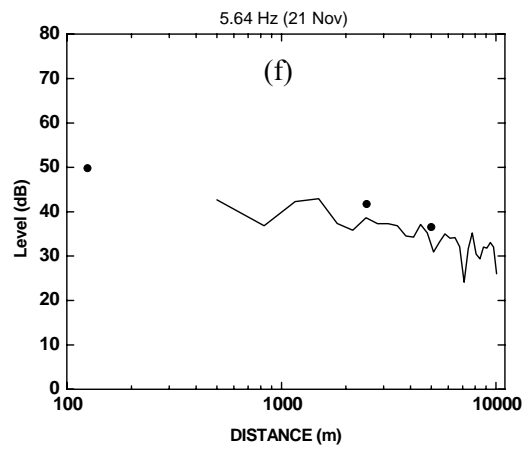
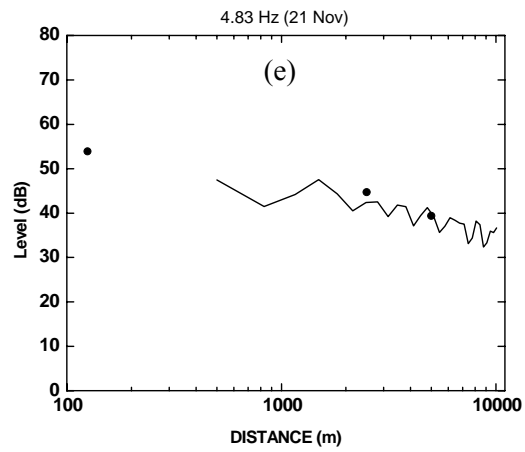
FIG. 53. Sound speed profile, 21 November 2013

This is the deepest inversion encountered thus far during the analysis of the measured results.

The predicted levels at 1.61 Hz, 2.42 Hz, 3.22 Hz, 4.03 Hz, 4.83 Hz, 5.64 Hz, 6.45 Hz, and 7.25 Hz are shown in the Figure 54 (a)-(h).







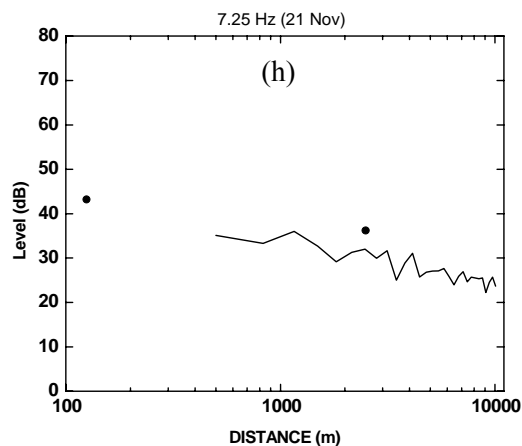


FIG. 54. Sound level variation with distance, prediction (lines) versus measurements (circles), 21 November 2013

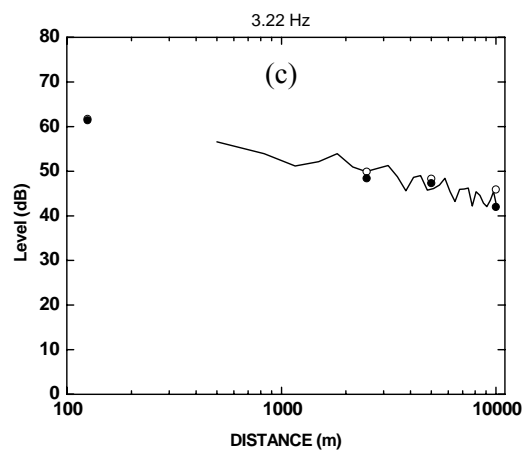
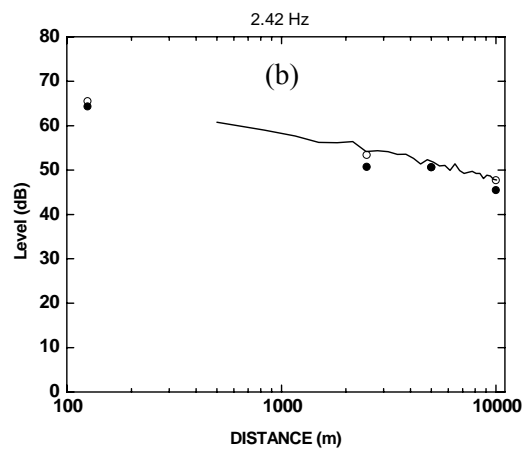
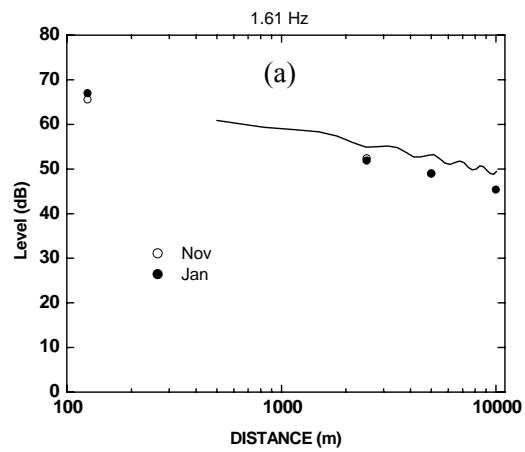
There is good agreement between measured and predicted levels at all frequencies. Further, despite the very deep inversion, these results compare well to those obtained during the other inversion conditions.

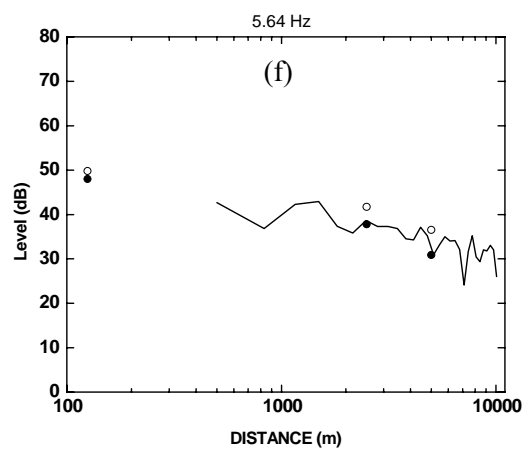
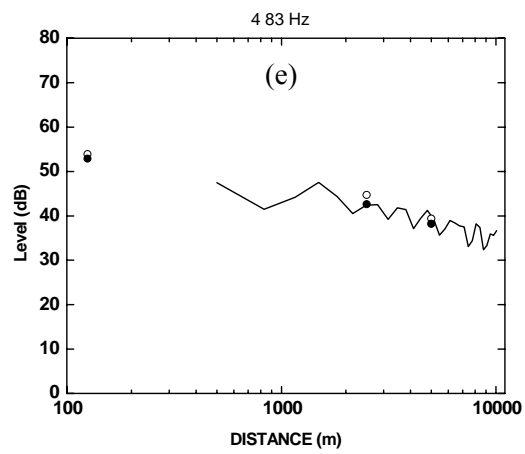
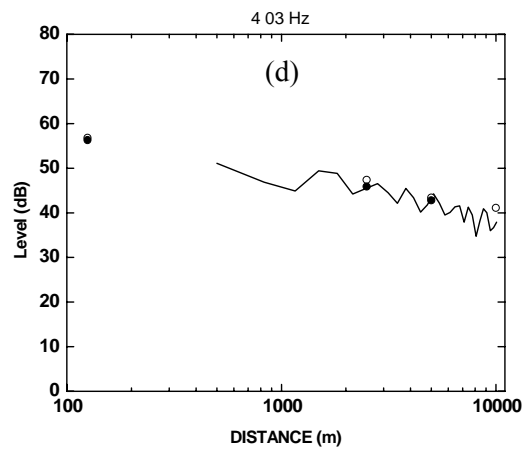
F. Analysis of January 2014 data

On January 2nd 2014 (03:00 to 04:00), the wind was blowing towards the SE with a speed of 6.4 m/s. The temperatures at 2 m and 10 m were -21.4°C and -19.4°C, respectively. This yields a sound speed profile virtually identical to the profile on November 21 2013.

During the Holiday Season, PEI received a significant amount of snowfall over several days. On January 2nd 2014, it is estimated that the island had an accumulation of close to 1 m of snow.

The predicted levels at 1.61 Hz, 2.42 Hz, 3.22 Hz, 4.03 Hz, 4.83 Hz, 5.64 Hz, and 6.45 Hz are shown in Figure 55 (a)-(g) below. The measured levels on January 2nd 2014 are plotted as the solid points. For comparison, the levels measured on November 21st 2013 are plotted as the open points.





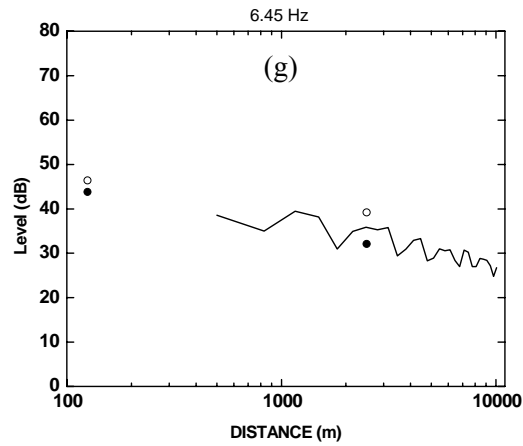


FIG. 55. Sound level variation with distance, prediction (lines) versus measurements (closed circles, 2 January 2014; open circles, 21 November 2013)

Despite the presence of snow covering the ground during the holiday season, the levels measured on January 2nd are generally the same as those measured on November 21st. We must conclude that whatever snow cover was present between HC1P and HC4P, it had no effect on the levels at these low infrasonic frequencies.

X. CONCLUDING REMARKS

Separating low-frequency wind turbine noise from the ambient background noise is a non-trivial challenge. The spectra of both are similar, rising at about 6 dB per octave as frequency decreases. As well, the overall level of both wind turbine and background noise increase in proportion to the wind speed. The only signals that can be unequivocally ascribed to the wind turbines are harmonically-related spectral peaks synchronous with the periodic passage of the turbine blades. Our propagation calculations have focused on these spectral peaks.

As general rule of thumb, the sound profile must be known to about 1/10 the propagation distance (admittedly, this rule has not been well-tested). However, similarity is only generally valid up to 1/10 of the boundary layer thickness (500 m to 2000 m). This generally limits the use of the similarity equations, for prediction of sound speed profiles, to heights below 100-200 m. Therefore, caution is required when using similarity for propagation distance greater than about 2 km.

We were able to successfully use the similarity equations in the cases studied thus far in Section IX up to a distance of 10 km. However, this cannot be generalized for other meteorological cases. For larger propagation distances (> 2 km), it is generally advisable to use data obtained from weather balloons, radar, sodar, etc.

We investigated an alternate approach to compute sound speed profiles, making use of archived Environment Canada weather data and the Harmonoise/Nord2000 weather classes. There was only limited success. For some combinations of stability, wind class and wind direction, the sound speed profile was similar to that derived from similarity theory using onsite meteorological measurements (which we take as being more rigorous), at least over the first 100 m or so of height. For other combinations, the profiles were not similar. At heights greater than 100 m, differences become progressively larger. We recommend that this approach be used only when no other information is available. An onsite meteorological station would be preferable, using its data and similarity theory to generate sound speed profiles up to 100 or 200 m. (And for heights above 200 m, something like a weather balloon should be used.) The Environment Canada data for cloud cover was actually too coarse to establish the stability class in all cases -- it may be better to make local observations.

Acoustic measurements made at three angular positions equidistant from wind turbine T2 were analyzed to assess the directivity of the turbine. Looking at the level of specific spectral peaks as a function of angle between wind and propagation directions does seem to suggest an effect. However, the strong dependence of the magnitude of these spectral peaks on the wind speed and the variability of ambient background noise make it difficult to be more conclusive. If there is some directivity associated with the low frequency spectral peaks, it is likely less than 5 dB. We had the impression that the spectral peaks rose and fell intermittently.

We were able to see clear spectral peaks at a number of infrasonic frequencies related to the blade passage frequency and its harmonics on several days between the months of June 2013 and January 2014. The levels of the spectral peaks were highest at 2.5, 5, and 10 km during various inversion and downwind conditions. No systematic differences in levels were observed between

the months of June and November during these meteorological conditions. By January 2nd 2014 it is estimated that PEI had an accumulation of nearly 1 m of snow. However, the levels of the spectral peaks on January 2nd showed no systematic difference with those measured during the other months in 2013.

XI. REFERENCES

- [1] report [REDACTED] found on the [REDACTED] website.
- [2] [REDACTED]
- [3] "Directivity of sound from wind turbines", KTH, The Marcus Wallenberg Laboratory for Sound and Vibration Research (Stockholm, 2011).
- [4] "Testing meteorological classifications for the prediction of long-term average sound levels", D. Heimann and E.M. Salomons, *Applied Acoustics* 65, 925-950 (2004).
- [5] Technical Report HAR29TR-041118-TNO10.pdf "Harmonoise WP2 Reference Model", written by E. Salomons and D. Heimann.
- [6] "Vertical sound speed profiles determined from meteorological measurements near the ground", D. Heimann, M. Bakermans, J. Defrance, and D. Kuhner, *Acta Acustica United with Acustica* 93, 228-240 (2007).